Universality of AC conduction in disordered solids

Dyre, J. C.; Schrøder, Thomas

Publication date:
1999

Document Version
Publisher's PDF, also known as Version of record

Citation for published version (APA):
Dyre, J. C., & Schrøder, T. (1999). *Universality of AC conduction in disordered solids*. Roskilde Universitet.

TEKST NR 376 1999

Universality of AC conduction in disordered solids

Jeppe C. Dyre
Thomas B. Schrøder

TEKSTER fra
IMFUFA ROSKILDE UNIVERSITETSCENTER
INSTITUT FOR STUDIET AF MATEMATIK OG FYSIK SAMT DERES FUNKTIONER I UNDERVISNING, FORSKNING OG ANVENDELSER

IMFUFA, Roskilde University, P.O.Box 260, 4000 Roskilde, Denmark

Universality of AC conduction in disordered solids

By: Jeppe C. Dyre and Thomas B. Schrøder

IMFUFA text nr. 376/99 37 pages ISSN 01066242

Abstract:

The striking similarity of AC conduction in quite different disordered solids is discussed in terms of experimental results, modeling, and computer simulations. After giving an overview of experiment a macroscopic and a microscopic model for AC conduction in disordered solids are reviewed. For both models the normalized AC conductivity as function of dimensionless frequency becomes independent of details of the disorder when the local randomly varying mobilities cover many orders of magnitude. The two "universal" AC conductivities are close to each other, but not identical. Three approximations for calculating the universal AC conductivities are presented and compared to computer simulations. It is argued that for both models AC universality reflects an underlying percolation determining DC as well as AC conductivity in the extreme disorder limit. Finally, model predictions are compared to experiment.

[Manuscript submitted to Reviews in Modern Physics]

Universality of AC conduction in disordered solids

Jeppe C. Dyre
Thomas B. Schrøder

Department of Mathematics and Physics, Roskilde University, DK-4000 Roskilde, Denmark

The striking similarity of AC conduction in quite different disordered solids is discussed in terms of experimental results, modeling, and computer simulations. After giving an overview of experiment a macroscopic and a microscopic model for AC conduction in disordered solids are reviewed. For both models the normalized AC conductivity as function of dimensionless frequency becomes independent of details of the disorder when the local randomly varying mobilities cover many orders of magnitude. The two "universal" AC conductivities are close to each other, but not identical. Three approximations for calculating the universal AC conductivities are presented and compared to computer simulations. It is argued that for both models AC universality reflects an underlying percolation determining DC as well as AC conductivity in the extreme disorder limit. Finally, model predictions are compared to experiment.

CONTENTS

I. INTRODUCTION

Though not generally appreciated, everyday "insulating" materials like glass or plastic have electrical properties remarkably in common. For one thing, the DC conductivity is always Arrhenius temperature-dependent. Our focus here, however, is on the strikingly universal AC properties: It is almost always possible to scale AC conductivity data at different temperatures into one single "master" curve. Different solids have so similar master curves that, for instance, electronic and ionic conduction cannot be distinguished. The only common feature of the numerous different solids exhibiting this *AC universality* is their disorder.

Not only disordered solids exhibit universal AC conductivity, so do extremely viscous liquids like ionic melts just above the glass transition. What causes AC universality? This question has been focus of interest ever since the full scope of AC universality was recognized in the 1970's (Isard, 1970; Namikawa, 1975; Jonscher, 1977; Owen, 1977; Mansingh, 1980). Recent results on ionic conductive glasses by Roling *et al.* (1997), Sidebottom (1999), and Ghosh and Sural (1999) have renewed interest in AC universality.

Below we review two simple models for AC conduction in disordered solids, a macroscopic model and a microscopic model. These models embody Occam's razor[1] by having essentially just one ingredient, disorder. Both models exhibit AC universality, i.e., in scaled units the AC conductivity becomes independent of the details of the disorder in the *extreme disorder limit* (when the local mobilities cover many orders of magnitude). The universal AC conductivities of the two models are rather similar and close to experiment. We show that for both models AC universality is caused by an underlying percolation dominating conduction in the extreme disorder limit. In this way universality, which for AC conduction has connotations different from its use in critical phenomena, is traced to percolation that *is* a critical phenomenon.

Why should nonspecialists care about the apparently esoteric subject of this Colloquium? One reason is the ubiquity of disordered materials - most likely there are several solids with universal AC conductivity in the very room you sit in. A second reason has to do with modeling. In modern condensed matter physics the extreme disorder limit is rarely considered. As we shall see, for AC conduction this limit leads to unusual non-power-law universalities. Similar universalities may very well occur elsewhere in "disordered" physics.

II. PRELIMINARIES

In this Section we recall the definitions of AC electrical conductivity and dielectric constant (see, e.g., Böttcher and Bordewijk (1978) or Reitz, Milford, and Christy (1993)). If $\mathbf{J}_{\rm tot}$ is "total" current density (with contribu-

[1] "It is vain to do with more what can be done with fewer" (Russell, 1946).

tions from bound as well as free charges) and $\mathbf{E}$ electric field the conductivity $\sigma_{\rm tot}$ is defined by $\mathbf{J}_{\rm tot} = \sigma_{\rm tot}\mathbf{E}$. In general the conductivity is frequency-dependent: If ω is the angular frequency $\sigma_{\rm tot}(\omega)$ is the complex quantity defined by $\mathbf{J}_{{\rm tot},0} = \sigma_{\rm tot}(\omega)\mathbf{E}_0$ where $\mathbf{J}_{\rm tot}(t) = {\rm Re}(\mathbf{J}_{{\rm tot},0}e^{i\omega t})$ and similarly for the electric field.

In a periodic field the complex frequency-dependent [relative] dielectric constant $\epsilon(\omega)$ is defined by $\mathbf{D}_0 = \epsilon(\omega)\epsilon_0\mathbf{E}_0$ where ϵ_0 is the vacuum permittivity and $\mathbf{D}_0$ the complex amplitude of the displacement vector $\mathbf{D} = \epsilon_0\mathbf{E}+\mathbf{P}$ ($\mathbf{P}$ being the dipole density). Since $\mathbf{J}_{\rm tot} = \dot{\mathbf{P}}$ conductivity and dielectric constant are related by $\sigma_{\rm tot}(\omega) = i\omega\,[\epsilon(\omega) - 1]\,\epsilon_0$. It follows that any solid with non-zero DC conductivity has the imaginary part of $\epsilon(\omega)$ diverging as frequency goes to zero. To avoid this $\sigma(0)$ is usually subtracted on the left hand side, leading to the following definition of $\epsilon(\omega)$ for a conducting solid,

$$\sigma_{\rm tot}(\omega) - \sigma(0) \;=\; i\omega\,[\epsilon(\omega) - 1]\,\epsilon_0. \qquad (1)$$

The negative imaginary part of $\epsilon(\omega)$ is referred to as the dielectric loss because, being given by the real part of the conductivity, it determines the dissipation.[2] The dielectric loss in disordered solids usually exhibits a peak, much like that characterizing dielectric relaxation in polar liquids (Böttcher and Bordewijk, 1978).

The AC conductivity includes contributions from both bound and free charges. It is generally believed that much below phonon frequencies ($\omega \ll 10^{12}$ Hz) - the frequencies of interest here - the bound charge polarization may be regarded as instantaneous.[3] This implies that the bound charge dielectric constant ϵ_∞ is frequency-independent. If $\sigma(\omega)$ denotes only the *free charge carrier* AC conductivity, we have $\sigma_{\rm tot}(\omega) = \sigma(\omega) + i\omega(\epsilon_\infty - 1)\epsilon_0$. The quantity $\sigma(\omega)$ is henceforth what we mean by "AC conductivity;" in terms of it Eq. (1) becomes

$$\sigma(\omega) - \sigma(0) \;=\; i\omega\,[\epsilon(\omega) - \epsilon_\infty]\,\epsilon_0\,. \qquad (2)$$

Writing $\sigma(\omega) = \sigma'(\omega) + i\sigma''(\omega)$, $\sigma''(\omega) \neq 0$ reflects a phase difference between field and free charge current. Below phonon frequencies, whenever the conductivity is frequency-dependent the charge carrier displacement always lags behind the electric field. This time-lag is at most one quarter of a period. The current consequently reaches its maximum *earlier* than the field, implying $\sigma''(\omega) > 0$. This reflects a capacitive response rather than an inductive. Of course, $\sigma'(\omega)$ is also positive because thermodynamics require positive dissipation.

[2]Recall that the average power absorbed per unit volume is ${\rm Re}\big(\sigma_{\rm tot}(\omega)\big)|\mathbf{E}_0|^2/2$.

[3]This is true only when one ignores secondary relaxations like those due to two-level tunneling systems important at very low temperatures.

III. AC CONDUCTION IN DISORDERED SOLIDS

Solids are classified into metals and non-metals. A metal has large weakly temperature-dependent DC conductivity, a non-metal has small DC conductivity which increases strongly with increasing temperature (Kittel, 1996). Only for non-metals is non-trivial AC conduction observed below phonon frequencies and only if the solid is somehow disordered. Examples of disordered non-metals with universal AC properties are ionic conductive glasses and melts (Owen, 1963; Angell, 1990; Kahnt, 1991; Roling, 1998), amorphous semiconductors (Owen, 1977; Mott and Davis, 1979; Long, 1982), polycrystalline semiconductors (Kuanr and Srivastava, 1994), electronic conductive polymers (Epstein, 1986; Jastrzebska, Jussila, and Isotalo, 1998), ionic conductive polymers (Rozanski *et al.*, 1995), transition metal oxides (Namikawa, 1975; Mansingh, 1980; Suzuki, 1980), metal cluster compounds (van Staveren, Brom, and de Jongh, 1991), organic-inorganic composites (Bianchi *et al.*, 1999), doped single crystal semiconductors at helium temperatures (where the disorder due to the random positions of the doping atoms becomes important) (Pollak and Geballe, 1961).

Figure 1 shows examples of AC data for six different disordered solids, three ionically conducting and three electronically conducting (the data in Fig. 1(b) are actually from an extremely viscous ionic melt just above the glass transition). Clearly, the AC conductivities are quite similar. There are hundreds, probably thousands, other examples like these. While ionic conduction is a classical barrier crossing process, electronic conduction in disordered solids usually proceeds via quantum mechanical tunneling between localized electron states. What do these conduction mechanisms have in common in disordered solids? The most likely answer is: very broad distributions of jump rates/tunneling rates/mobilities (Dyre, 1988; Elliott, 1990). Below we study two models with such broad distributions and find that they largely reproduce experiment.

AC universality was first discovered for ionic conductive classical oxide glasses. Taylor (1956, 1957, 1959) showed that the dielectric loss for different glasses falls on a single plot against scaled frequency. He also noted that the activation energy of the DC conductivity is always the same as that of the frequency marking onset of AC conduction. Subsequently,[4] Isard (1961) relabeled Taylor's axis by plotting dielectric loss against log of the product of frequency and resistivity, thus essentially arriving at AC scaling in the form

[4]Owen (1963) gave an excellent review of early works on DC and AC properties of ionic conductive glasses.

$$\tilde{\sigma} \equiv \sigma(\omega)/\sigma(0) = F\left(C\frac{\omega}{\sigma(0)}\right) . \qquad (3)$$

Since then Eq. (3), which we shall refer to as "Taylor-Isard scaling," has been used in several different contexts by authors often unaware of the pioneering works of Taylor and Isard. For instance, Taylor-Isard scaling was used by Scher and Lax (1973) in their famous papers introducing the continuous time random walk approximation, by Summerfield (1985) and Balkan *et al.* (1985) for amorphous semiconductors, and by van Staveren, Brom, and de Jongh (1991) for metal-cluster compounds. For ionic conductive glasses Taylor-Isard scaling was used more recently, e.g., by Kahnt (1991), Kulkarni, Lunkenheimer, and Loidl (1998), and Roling (1998).

Three examples of Taylor-Isard scaling are shown in Fig. 2. The figures 2(a) and 2(b) give the master curves for the data shown in Figs. 1(a) and 1(d) respectively. Figure 2(c) shows the common master curve for eight different ionic conductive glasses. The three master curves of Fig. 2 are similar, but not identical (the Fig. 2(b) curve is slightly steeper than the two others). In all three examples the authors chose to fix the Taylor-Isard scaling constant C to be proportional to $1/T$. As shown below (Eq. (7)), in general $C \propto \Delta\epsilon$ where $\Delta\epsilon = \epsilon(0) - \epsilon_\infty$; thus choosing $C \propto 1/T$ corresponds to assuming a Curie-law for $\Delta\epsilon$. The Curie-law, however, is not always obeyed (Namikawa, 1975; Sidebottom, 1999) so possibly even "better" master curves would have been arrived at if no Curie-law was assumed.

We now proceed to list the AC characteristics of disordered solids (Dyre, 1988). When reading the first 11 points below it may be helpful to compare to Figs. 1 and 2.

1. The real part of the AC conductivity increases with frequency, the imaginary part is non-negative.
2. At high frequencies $\sigma'(\omega)$ apparently follows a power-law,
$$\sigma'(\omega) \propto \omega^n . \qquad (4)$$
3. Deviations from a power-law always correspond to n increasing weakly with frequency.
4. n is between[5] 0.6 and 1.0.
5. In a fixed frequency range n increases as temperature decreases and $n \to 1.0$ for $T \to 0$.
6. When there is no measurable DC conductivity n is close to 1.0.
7. At low frequencies there is a gradual transition to frequency-independent conductivity.
8. In a log-log plot $\sigma'(\omega)$ is much less temperature-dependent than $\sigma(0)$.
9. At temperatures so low that n is close to 1.0 $\sigma'(\omega)$ is almost temperature-independent.
10. The shape of $\sigma'(\omega)$ in a log-log plot is temperature-independent, i.e., AC conductivity obeys the *time-temperature superposition principle* making it possible to construct a master curve.
11. The shape of the master curve is roughly the same for all disordered solids.
12. Whenever $\sigma(0)$ is measurable there is a dielectric loss peak.
13. The onset of AC conduction takes place around the dielectric loss peak frequency ω_m.
14. ω_m satisfies the Barton-Nakajima-Namikawa relation (Barton, 1966; Nakajima, 1972; Namikawa, 1975)
$$\sigma(0) = p\,\Delta\epsilon\,\epsilon_0\,\omega_m , \qquad (5)$$
where p is a numerical constant of order one. Experimental evidence for Eq. (5) is reproduced in Fig. 3.
15. The dielectric loss strength $\Delta\epsilon$ is much less temperature-dependent than ω_m or $\sigma(0)$, so Eq. (5) implies the rough proportionality
$$\sigma(0) \sim \omega_m . \qquad (6)$$
16. $\sigma(0)$ and ω_m are Arrhenius temperature-dependent with same activation energy.

Is not the time-temperature superposition principle inconsistent with the finding that n depends on temperature? In principle yes, but in practice no because the power-law description is only approximate: If temperature is lowered the master curve is displaced to lower frequencies (Fig. 1). At the same time one observes $n \to 1.0$ for measurements performed in a fixed frequency range. We conclude that the slope of the master-curve - instead of being constant as for an exact power-law - goes to one as scaled frequency goes to infinity.[6]

---

[5] In practice the determination of n depends somewhat on the width of the frequency-range studied.

[6] This applies far below phonon frequencies. Around phonon frequencies there are various resonance phenomena and at even higher frequencies $\sigma'(\omega)$ goes to zero fast enough that $\int_0^\infty \sigma'(\omega)d\omega$ is finite (Kubo, 1957).

The time-temperature superposition principle makes it possible to determine the Taylor-Isard scaling constant C of Eq. (3) and derive the Barton-Nakajima-Namikawa relation. We first show (Sidebottom, 1999; Schrøder and Dyre, 1999) that

$$\tilde{\sigma} \;=\; F\left(\frac{\Delta\epsilon\;\epsilon_0}{\sigma(0)}\;\omega\right). \qquad (7)$$

Assuming the existence of a temperature-independent function $\tilde{\sigma}(\tilde{\omega})$ where $\tilde{\omega}$ is the scaled frequency, we expand $\tilde{\sigma}$ to first order: $\tilde{\sigma} = 1 + i\tilde{\omega}A$, where A is real because $\sigma^*(\omega) = \sigma(-\omega)$. Since $\sigma = \tilde{\sigma}\sigma(0)$ we have $\sigma(\omega) = \sigma(0) + i\tilde{\omega}A\sigma(0)$. On the other hand, $\Delta\epsilon$ obeys $\sigma(\omega) = \sigma(0) + i\omega\Delta\epsilon\epsilon_0$ for $\omega \to 0$ (Eq. (2)), and consequently $\tilde{\omega} = A^{-1}[\Delta\epsilon\epsilon_0/\sigma(0)]\,\omega$. This finishes the proof (Schrøder and Dyre, 1999). Once Eq. (7) has been established, the Barton-Nakajima-Namikawa relation Eq. (5) is derived as follows: Equation (2) implies $\epsilon(\omega) - \epsilon_\infty \propto (\tilde{\sigma} - 1)/\tilde{\omega}$. This is a function of $\tilde{\omega}$ and thus the dielectric loss has its maximum at some particular temperature-independent value of $\tilde{\omega}$. Denoting this by $\tilde{\omega}_m$ we have (from the above reasoning) $\tilde{\omega}_m = A^{-1}\,[\Delta\epsilon\epsilon_0/\sigma(0)]\;\omega_m$, so if $p \equiv 1/A\tilde{\omega}_m$ we get $1/p = [\Delta\epsilon\epsilon_0/\sigma(0)]\;\omega_m$ which is the required Eq. (5). The only thing we cannot prove, of course, is the experimental finding that p is never far from one (Namikawa, 1975). - In practice the scaling expressed by Eq. (7) simply means that frequency is scaled such that the imaginary part of $\tilde{\sigma}$ is equal to scaled frequency as $\omega \to 0$.

We finally note that there *are* exceptions to the above 15 points. There are solids where n is slightly larger than 1.0 (Lakatos and Abkowitz, 1971; Lim, Vaysleyb, and Nowick, 1993; Durand *et al.*, 1994). There are solids where the DC conductivity is not Arrhenius, notably group-IV amorphous semiconductors (Mott and Davis, 1979). Finally, in some cases the conductivity is weakly frequency-dependent much below ω_m (Jonscher, 1996). In our view these are rare and insignificant exceptions to the overall experimental picture, but this viewpoint is not universally accepted. Thus Elliott (1994), Macdonald (1997), and Ngai and Moynihan (1998) all emphasize the *differences* between various disordered solids. On the other hand, an experienced experimentalist in this field recently discontinued AC measurements because "we always see more or less the same" (Kremer, 1999). Why is that? Is there any simple way of understanding AC universality? These are the main questions we address below, ignoring the minor variations between different disordered solids.

IV. MACROSCOPIC MODEL

The first model we consider assumes the disorder is present only on a macroscopic scale. In that case the concept of a local conductivity makes sense and Maxwell's equations may be applied to find the AC conductivity.

A. Definition

Any solid consisting of phases with different conductivity has an overall conductivity which increases with frequency (Maxwell, 1891; Wagner, 1913). This is because at high frequencies localized charge carrier motions make it possible to take maximum advantage of well conducting regions, while at lower frequencies charge transport must extend over longer distances and is limited by bottlenecks of less well conducting regions. The proper way to study this phenomenon is to apply Maxwell's equations to the inhomogeneous solid. In a solid with spatially varying frequency-independent free charge conductivity $g(\mathbf{r})$ but constant bound charge dielectric constant we have, if $\mathbf{J}$ is the free charge current density, $\mathbf{J}(\mathbf{r},t) = g(\mathbf{r})\mathbf{E}(\mathbf{r},t)$ and $\mathbf{D}(\mathbf{r},t) = \epsilon_\infty\epsilon_0\mathbf{E}(\mathbf{r},t)$. Combining these equations with a) the definition of the electrostatic potential ϕ, b) Gauss' law, and c) the continuity equation, one arrives at the following equation for ϕ in a periodic field (Fishchuk, 1986; Dyre, 1993)

$$\nabla\cdot\Big(\;[i\omega\,\epsilon_\infty\epsilon_0 + g(\mathbf{r})]\;\nabla\phi\;\Big) \;=\; 0\,. \qquad (8)$$

When Eq. (8) is discretized one arrives at the circuit shown in Fig. 4 (Dyre, 1993). All capacitors are equal, proportional to ϵ_∞, while the resistors are proportional to the local resistivity $1/g(\mathbf{r})$. The interpretation of the circuit seems straightforward at first: Resistor currents are free charge currents and capacitor currents are bound charge currents. If that were correct, however, according to Kirchhoff's current law there could be no charge accumulation anywhere in the solid. In reality the capacitor currents are *Maxwell's displacement currents* - the capacitors would be there even in absence of bound charges (Dyre, 1993).

How does one extract the overall AC conductivity from the circuit? Imagine each of two opposing faces short-circuited to act as electrodes and a periodic potential applied. The average resistor current determines the free charge AC conductivity $\sigma(\omega)$. If the admittance between the electrodes is $Y(\omega)$, L is the linear circuit dimension, and d is the dimension, $\sigma(\omega)$ is found by subtracting the capacitor contribution (Fishchuk, 1986; Dyre, 1993):

$$\sigma(\omega) \;=\; \frac{Y(\omega)}{L^{d-2}} \;-\; i\omega\,\epsilon_\infty\epsilon_0. \qquad (9)$$

Note that the frequency-dependence of σ is not due to the (subtracted) direct capacitor contribution to the overall admittance. Instead, $\sigma(\omega) \neq \sigma(0)$ because the capacitors influence the node potentials which determine the resistor currents.

To realistically model a disordered non-metal the local free charge conductivity is taken to be Arrhenius temperature-dependent, $g = g_0 \exp(-\beta E)$ where $\beta = 1/k_B T$ and E is the so-called activation energy. Conduction may be classical or quantum mechanical, it does not matter. The solid disorder is reflected in $g = g(\mathbf{r})$ being somehow random.[7] Any random function has a correlation length beyond which values are essentially uncorrelated. If the discretization length is equal to this correlation length it makes good sense to assume the resistors are uncorrelated from link to link (Kirkpatrick, 1973). After this simplification the model is uniquely defined by the activation energy probability distribution $p(E)$.

In one dimension the circuit is a series of RC-elements and the calculation of $Y(\omega)$ is straightforward. In particular, the circuit impedance at zero frequency is the sum of the individual resistors, implying (Dyre, 1993) $\sigma(0) = \langle g^{-1} \rangle^{-1}$. In more than one dimension the calculation of $\sigma(\omega)$ involves solving Kirchhoff's circuit equations which cannot be done analytically, even in the DC limit. In the high frequency limit, however, the capacitor admittances are so large that they completely dominate, resulting in a spatially homogeneous electric field. Consequently, the average resistor current is determined by the spatially averaged free charge conductivity. This leads to $\sigma(\infty) = \langle g \rangle$ (Dyre, 1993). Summarizing the exact results,

$$\begin{aligned} d = 1 &: \ \sigma(0) \ = \ \langle g^{-1} \rangle^{-1} \ , \\ d \geq 1 &: \ \sigma(\infty) = \langle g \rangle \ . \end{aligned} \tag{10}$$

B. AC universality in extreme disorder limit

If temperature is lowered β increases and the local conductivities cover more and more decades - eventually what we term the "extreme disorder limit" is approached (Shklovskii and Efros, 1984; Tyč and Halperin, 1989). Although it is not obvious *a priori* that anything interesting happens in this limit, we shall see that the AC conductivity in scaled units becomes independent of both β and $p(E)$. This is *AC universality* as the term is used here for models. No rigorous mathematical proof of AC universality exists, but there is convincing evidence from three sources: 1) AC universality is predicted by the effective medium approximation; 2) AC universality is found in computer simulations; and 3) it is possible to physically understand the origin of AC universality. Points 1) and 2) are considered below for the macroscopic model and in Section V for the symmetric hopping model, point 3) is discussed in Section VI for both models.

To find $\sigma(\omega)$ we need to calculate the overall admittance of a circuit of randomly varying admittances y (Fig. 4). This problem cannot be solved analytically so we use the effective medium approximation (EMA), a standard technique for calculating average physical properties of random mixtures. The idea is to focus on one small part of the mixture and regard it as embedded in an effective medium with the average property. Then selfconsistency is required such that, on the average, the embedding in the effective medium has the same overall property as the effective medium itself. This approximation was first used by Bruggeman (1935) for calculating the dielectric constant of mixtures of dielectrics and for calculating the thermal and DC electrical conductivity of mixtures. The effective medium approximation may also be used, e.g., for calculating the bulk or shear modulus of a mixture of solids with different elastic properties (Berryman, 1980) or, as in the next Section, the AC conductivity of a hopping model. The idea has also been used in quantum mechanics for calculating the average one-particle Green's function for a disordered system, here termed the "coherent potential approximation" (Economou, 1983).

According to the effective medium approximation for a random admittance network in d dimensions the overall circuit admittance is the same as that of a circuit of equal admittances y_m, where y_m is the solution (Kirkpatrick, 1973) of

$$\left\langle \frac{y - y_m}{y + (d-1)\, y_m} \right\rangle \ = \ 0 . \tag{11}$$

The brackets indicate averaging over the admittance probability distribution. Just sketching how Eq. (11) is applied to the macroscopic model, one substitutes the admittance of each RC-element of Fig. 4, $y \propto g(\mathbf{r}) + i\omega\epsilon_\infty\epsilon_0$, into Eq. (11) (where y_m depends on frequency). Equation (9) translates into $y_m \propto \sigma(\omega) + i\omega\epsilon_\infty\epsilon_0$ and the following equation for $\sigma = \sigma(\omega)$ is arrived at (Fishchuk, 1986; Dyre, 1993):

$$\left\langle \frac{g - \sigma}{g + (d-1)\, \sigma + d\, i\omega\, \epsilon_\infty \epsilon_0} \right\rangle \ = \ 0 . \tag{12}$$

For $\omega \to \infty$ Eq. (12) correctly implies $\sigma(\infty) = \langle g \rangle$ (Eq. (10)) because at very large frequencies the denominator varies little and may be regarded as constant. In one dimension the DC conductivity is also correctly predicted by Eq. (12).

It is possible to solve Eq. (12) in the extreme disorder limit. In terms of a suitably defined dimensionless frequency $\tilde{\omega}$, independent of $p(E)$ the normalized AC conductivity $\tilde{\sigma}$ (Eq. (3)) is the solution (Dyre, 1993) of

$$\tilde{\sigma} \, \ln \tilde{\sigma} \ = \ i\tilde{\omega} . \tag{13}$$

---

[7] A disordered solid is rarely random in the mathematical sense (Ziman, 1979). We here follow what has become the standard approach, namely to replace complexity by randomness. The rationale for doing this has been beautifully summarized by Wolynes (1992).

The universality of this equation was only recognized several years after it first appeared in the literature. The equation was originally derived as the solution of a hopping model describing a dilute system of electrons tunneling between states randomly localized in space (Bryksin, 1980; Böttger and Bryksin, 1985). Subsequently, Fishchuk (1986) derived Eq. (13) for the macroscopic model with "Box" activation energy distribution ($p(E)$ flat with sharp cut-off's), and Eq. (13) was derived for symmetric hopping also with the Box distribution (Dyre, 1988).

The effective medium approximation universality equation Eq. (13) is easy to solve numerically. Accurate analytical approximations are available (Dyre, 1993); it is even possible to give an explicit integral representation of $\tilde{\sigma}(\tilde{\omega})$ (Dyre and Jacobsen, 1995). The solution is constant at low frequencies ($\tilde{\omega} \ll 1$), while at high frequencies ($\tilde{\omega} \gg 1$) the real part of the conductivity follows an approximate power-law with exponent $n < 1$ which goes slowly to one as $\tilde{\omega} \to \infty$ (Böttger and Bryksin, 1985; Dyre, 1988).

Do the effective medium predictions hold? Figure 5 reproduces two examples of the simulations carried out in two dimensions by Dyre (1993). For simplicity, only *imaginary* frequencies (denoted by s) were used in these simulations. This is a technical trick - at imaginary frequencies all numbers become real because the capacitor admittances are real, simplifying calculations considerably. In Fig. 5(a) results for one activation energy distribution at different β's are given, clearly converging to universality as $\beta \to \infty$. The full curves show the predictions of the effective medium approximation. Similar figures exist for other distributions. Figure 5(b) shows the AC conductivity of different distributions at high β's. All distributions lead to the same AC conductivity which is well represented by Eq. (13) (full curve). A few three-dimensional simulations were also presented in Dyre (1993), but only going to β=60. The best three-dimensional simulations available today are probably those of Dyre and Riedel (1994) using an iterative technique, finding again very good agreement with Eq. (13) in the extreme disorder limit. In conclusion, the effective medium approximation universality equation (13) quite well describes the universal AC conductivity of the macroscopic model.

V. SYMMETRIC HOPPING MODEL

The macroscopic model does not apply for solids strongly disordered on the atomic scale. Below we review results for a highly idealized hopping model with microscopic disorder. This model is physically quite different from the macroscopic model. It does not take Coulomb interactions into account - instead the electric field is assumed to be spatially homogeneous. Despite these differences the AC predictions of the two models are rather similar.

A. Definition

The term "hopping" refers to sudden displacement of a charge carrier from one position to another, usually just Ångstroms away. The simplest hopping model has non-interacting charge carriers placed on a cubic lattice with only nearest-neighbor jumps allowed. It is assumed that the jump rates (jump probabilities per unit time) are symmetric, i.e., the same for jumps up and down. According to the principle of detailed balance - a consequence of microscopic time-reversibility - jump rates are symmetric whenever all lattice sites are equally probable (van Kampen, 1981).

Each jump rate is given (Lidiard, 1957) by $\Gamma = \gamma_0 \exp(-\beta E)$ where γ_0 is the so-called attempt frequency and $\beta = 1/k_B T$.[8] The activation energy E (the barrier to be overcome) is assumed to vary randomly. Figure 6 illustrates a one-dimensional example of the kind of potential leading to the symmetric hopping model. The more general asymmetric hopping model has been studied in other contexts like protein dynamics or viscous liquid flow (see, e.g., Stein and Newman (1995) or Dyre and Jacobsen (1995) and their references).

Our main motivation for studying the symmetric hopping model is that it is the simplest model with microscopic disorder and realistic AC predictions. The model however may seem completely unrealistic. It ignores the fact that charge carriers repel each other. Also, it allows an arbitrary number of charge carriers at each site, but in reality - whether these are ions or localized electrons - there is room for just one charge carrier at each site. Finally, one expects energies to vary from site to site. A more realistic model has randomly varying site energies and allows only jumps to vacant sites. If this "Fermi model" is linearized with respect to an external electric field, however, the result is mathematically equivalent to the symmetric hopping model (Böttger and Bryksin, 1985). Although the linearization replaces the 0-1 occupation number by a continuous variable - a non-trivial approximation (Shklovskii and Efros, 1984) - this result shows that the symmetric hopping model is not totally unrealistic[9] although, of course, it still ignores Coulomb

[8] For simplicity only hopping *over* a barrier is considered, but the model applies also for quantum mechanical tunneling of localized electrons, in which case β is not inverse temperature but inverse wavefunction size.

[9] In particular, the symmetric hopping model also describes tunneling of non-iso-energetic electrons (Elliott, 1990).

repulsions.

Because the charge carriers are assumed non-interacting it is enough to consider the motion of one single charge carrier. All information about this motion is contained in the so-called *master equation* for the probability to find the charge carrier at lattice site s, $P_{\mathbf{s}}$ (van Kampen, 1981). If $\Gamma(\mathbf{s},\mathbf{s}')$ is the rate of jumps between s and s' (non-zero only for nearest neighbors) the hopping master equation (Kimball and Adams, 1978; Böttger and Bryksin, 1985; Haus and Kehr, 1987; Stein and Newman, 1995; Hughes, 1996) is

$$\frac{d}{dt}P_{\mathbf{s}} \;=\; \sum_{\mathbf{s}'}\Gamma(\mathbf{s},\mathbf{s}')\,(P_{\mathbf{s}'}-P_{\mathbf{s}})\,. \tag{14}$$

Anyone who feels uncomfortable thinking about a time-dependent probability for one single charge carrier may instead imagine numerous (non-interacting) charge carriers hopping all over the lattice and *define* $P_{\mathbf{s}}$ as the number of charge carriers at site s relative to the total number. With this interpretation Eq. (14) describes the rate of change of average site occupations.

Equation (14) applies when there is no external electric field. In a non-zero field jumps in the field direction are favored. The result is a net current. The *fluctuation-dissipation theorem* expresses the frequency-dependent conductivity in terms of the equilibrium (zero-field) current auto-correlation function (Kubo, 1957; Becker, 1967). If q is charge and n charge carrier concentration, the fluctuation-dissipation theorem for a system of non-interacting charge carriers (Scher and Lax, 1973) is

$$\sigma(\omega) = \frac{nq^2}{k_BT}\,D(\omega)\,, \tag{15}$$

where the frequency-dependent diffusion constant $D(\omega)$ is defined as the Laplace transform of the velocity auto-correlation function (v being the velocity in any fixed direction):

$$D(\omega) \;=\; \int_0^\infty \langle v(0)v(t)\rangle\; e^{-i\omega t}\,dt\,, \tag{16}$$

How is velocity defined for a charge carrier that sits still most of the time and jumps in principle infinitely fast when it moves? The answer is that the velocity is a sum of delta-functions. This causes no problems - in fact the velocity auto-correlation function has a $\delta(t)$-term, but is otherwise continuous. A simple example is when all jump rates are equal. Then jumps are uncorrelated and the velocity auto-correlation function is zero for $t > 0$, thus proportional to $\delta(t)$. In this case, $D(\omega)$ is constant and Eq. (15) implies the conductivity is frequency-independent.

Kimball and Adams (1978) proved that for any hopping model

$$\sigma(\omega) = \sigma(\infty) - \sum_n \frac{A_n}{\gamma_n + i\omega}\,, \tag{17}$$

where $A_n \geq 0$ and $\gamma_n \geq 0$. From this a number of important conclusions may be drawn (the first two may be proved also for the macroscopic model): 1) $\sigma'(\omega)$ is an increasing function of frequency; 2) $\sigma''(\omega)$ is non-negative; 3) by inverse Laplace transform Eqs. (15), (16), and (17) imply that for $t > 0$

$$\langle v(0)v(t)\rangle \;\leq 0\,. \tag{18}$$

In terms of the mean-square displacement $\langle \Delta x^2(t)\rangle$ Eq. (18) implies[10] that for $t > 0$

$$\frac{d^2}{dt^2}\,\langle \Delta x^2(t)\rangle \;\leq\; 0\,. \tag{19}$$

Figure 7 illustrates these results. Why is the velocity auto-correlation function negative? First, note that from any site the most likely jump is along the link with largest jump rate. The next jump is more likely to go back again than to any other site, simply because the link just jumped along generally has large jump rate (compare Fig. 6). This "bounce-back effect" (Kimball and Adams, 1978; Funke, 1993) results in the velocity auto-correlation function being negative and consequently in Eq. (19).

We shall adopt the "rationalized" unit system in which conductivity and diffusion constant are both normalized such that on a homogeneous lattice with link jump rate Γ one has $\sigma = D = \Gamma$. In analogy to Eq. (10) for the macroscopic model there are two exact results for the symmetric hopping model (Alexander *et al.*, 1981),

$$\begin{aligned} d = 1:\;\; \sigma(0) \;&=\; \langle \Gamma^{-1}\rangle^{-1}\,, \\ d \geq 1:\;\; \sigma(\infty) &= \langle \Gamma\rangle\,. \end{aligned} \tag{20}$$

Calculating the AC conductivity analytically is not possible so, just as for the macroscopic model, one resorts to approximations and computer simulations.

B. AC universality in extreme disorder limit

As already mentioned, there is also an effective medium approximation for the symmetric hopping model. If $s\tilde{G}$ is the following integral

$$s\tilde{G} \;=\; \int_{-\pi<k_i<\pi} \frac{d\mathbf{k}}{(2\pi)^d}\,\frac{i\omega}{i\omega + 2\,\sigma\,[d - \sum_i \cos \mathrm{k}_i]}\,, \tag{21}$$

---

[10] Squaring and averaging $\Delta x(t) = \int_0^t v(t')dt'$ one arrives at $\langle \Delta x^2(t)\rangle = \int_0^t dt' \int_0^t dt''\,\langle v(t')v(t'')\rangle$, which implies $d^2/dt^2\,\langle \Delta x^2(t)\rangle = 2\,\langle v(0)v(t)\rangle$ for $t > 0$.

the effective medium approximation self-consistency equation for $\sigma = \sigma(\omega)$ (Haus and Kehr, 1987) is

$$\left\langle \frac{\Gamma - \sigma}{\Gamma + (d-1)\,\sigma + s\tilde{G}\,(\sigma - \Gamma)} \right\rangle = 0\,. \qquad (22)$$

The brackets denote an averaging over the jump rate probability distribution. It is easy to show that Eq. (22) implies the two exact results Eq. (20).

Equation (22) may be solved in the extreme disorder limit ($\beta \to \infty$). The calculations are more involved than for the macroscopic model, but the result is the same (Dyre, 1994): In terms of dimensionless frequency $\tilde{\omega}$, $\tilde{\sigma}(\tilde{\omega})$ obeys the effective medium approximation universality equation (13). The case $d = 2$ is marginal and requires special treatment, eventually leading again to Eq. (13). Below two dimensions the effective medium approximation does *not* lead to Eq. (13), a fact which becomes important in the next section.

Figure 8 shows results of computer simulations of the symmetric hopping model. Figure 8(a) gives the AC conductivity as function of frequency in non-scaled units for the Box distribution of activation energies at different temperatures. Figure 8(b) shows the convergence to universality as $\beta \to \infty$ for the data of Fig. 8(a) scaled according to Eq. (7). Finally, Fig. 8(c) shows the large-β AC conductivities for 5 different $p(E)$'s, clearly showing universality. In Fig. 8(c) the full line shows the effective medium approximation universality prediction Eq. (13) which is not accurate. In two dimensions this approximation is even less accurate (Dyre, 1994).

VI. CAUSE OF UNIVERSALITY

We have seen that two physically quite different models both have AC universality in the extreme disorder limit. The obvious question now is: What causes AC universality? Below we give our answer to this question, presenting a physical picture of conduction in the extreme disorder limit. The scenario outlined builds on well-known insights gained during the last 30 years, but some of it is new and more speculative. From this physical picture two approximations for calculating the universal AC conductivity (in either model) are arrived at.

A. Role of percolation

We shall argue that in both models AC universality arises because percolation controls the conductivity in the extreme disorder limit. First, let's briefly recall what percolation is (Broadbent and Hammersley, 1957; Isichenko, 1992; Stauffer and Aharony, 1992). Consider a cubic lattice in any dimension and suppose each link is randomly marked with probability p (Fig. 9). When p is low few links are marked and clusters of connected marked links are small. Increasing p the average cluster size increases. At the so-called percolation threshold p_c an infinite cluster appears, the "percolation cluster." In two dimensions $p_c = 0.5$ exactly, in three dimensions $p_c \cong 0.2488$ (Isichenko, 1992).

We first show how the DC conductivity activation energy E_c for both models is determined from percolation arguments. In the DC limit the macroscopic model is described by a simple resistor network (compare Fig. 4 where the capacitors carry no DC currents). The current prefers the path of least resistance. When β is large the random resistors cover many decades. Imagine now the resistors marked in order of increasing resistance. A DC current is possible through marked resistors only when the fraction of marked resistors exceeds p_c. When this happens, due to large spread of resistors, marking more resistors does not significantly change the admittance of the set of marked resistors. This admittance is dominated by the largest resistors among the marked right at percolation. Consequently, the DC conductivity activation energy E_c is equal to that of the "bottleneck" resistors, given by

$$\int_0^{E_c} p(E)\,dE = p_c\,. \qquad (23)$$

Equation (23) was first derived by the above physical arguments (Ambegaokar, Halperin, and Langer, 1971; Shklovskii and Efros, 1971; Kirkpatrick, 1973), but later proved rigorously (Tyč and Halperin, 1989).

The DC conductivity activation energy for symmetric hopping is also given by Eq. (23): The main contribution to the mean-square displacement comes from charge carriers utilizing the links with largest jump rates. To do this at long times and extend the motion to infinity, optimal charge carriers move preferably on the percolation cluster. Here, they must every now and then overcome the barrier E_c given by Eq. (23), the largest barrier on the percolation cluster. At large β these barriers act as bottlenecks and consequently E_c determines the rate of mean-square displacement. Via Einstein's equation $\langle \Delta x^2(t) \rangle = 2Dt$ and the fluctuation-dissipation theorem (Eq. (15), here used at zero frequency) we conclude that the activation energy of $\sigma(0)$ is given by Eq. (23).[11]

[11] Another way to prove this is to utilize that hopping in the DC limit is described by a resistor circuit. As shown by Miller and Abrahams (1960) in steady state the master equation Eq. (14) may be identified with Kirchhoff's current law if probability is identified with potential and jump rate with inverse resistance. The large spread of jump rates as $\beta \to \infty$ is translated into a large spread of resistors. In this way the above derivation of Eq. (23) for the macroscopic model applies to the symmetric hopping model as well.

Before proceeding to discuss the origin of AC universality we must look a bit more closely on where the DC current flows. The problem is that the percolation cluster is a mathematical fractal (Staffer and Aharony, 1992) and as such has zero bulk DC conductivity (Bouchaud and Georges, 1990). Thus besides the percolation cluster a tiny extra fraction of resistors *must* also be involved in carrying the DC current. Enlarging the percolation cluster to include these extra resistors gives us a set we term the "fat" percolation cluster. How large is the fat percolation cluster? In addition to the exact percolation cluster one only expects that it involves extra links with activation energies a few k_BT above E_c - adding more links cannot change the conductivity significantly since these links conduct poorly anyway. Note that in the extreme disorder limit the fat percolation cluster converges to the exact percolation cluster and the proof that E_c is given by Eq. (23) still holds. The arguments given below for AC universality in the extreme disorder limit rest on the assumption that not only DC, but also AC conduction (at frequencies where AC universality applies) mainly takes place on the fat percolation cluster. We thus assume that AC contributions from finite isolated "islands" are unimportant. At this point we differ from previous attempts to relate AC conductivity to the underlying percolation (Böttger and Bryksin, 1985; Hunt, 1995).

Turning now to the origin of AC universality we first ask, starting by the macroscopic model: Why is conductivity frequency-independent at low frequencies and what determines the onset of AC conduction? To answer these questions, recall that all capacitors in Fig. 4 are equal. At very low frequencies each capacitor has smaller admittance than its partner-resistor. The circuit current flows in the resistors and, viewed from the electrodes, the circuit looks like a simple resistor circuit. If frequency is increased an increasing number of capacitor admittances become numerically larger than their resistor-partner. Whenever this happens for a link we term it "affected." Although an increasing number of links are affected, the average resistor current changes only insignificantly as long as none of the affected links are on the fat percolation cluster. Increasing frequency further, however, at some point links on the fat percolation cluster become affected. The first of these are the bottlenecks. Increasing frequency even further affects more and more links on the fat percolation cluster: The node potentials on this set (carrying the main resistor currents) change, therefore do the resistor currents. Clearly, the frequency marking onset of AC conduction is proportional to the DC conductivity, because both are determined by the bottleneck admittance. We thus arrive at Eq. (6), the Barton-Nakajima-Namikawa relation's rough proportionality between DC conductivity and dielectric loss peak frequency (the latter marking onset of AC conduction).

For a fixed range of frequencies around ω_m the resistors of the affected links on the fat percolation cluster cover a corresponding range. As $\beta \to \infty$ these involve only a very narrow range of activation energies around E_c. Consequently, the AC behavior in the fixed frequency range is determined by just the *number* $p(E_c)$. The scaled conductivity $\tilde{\sigma}$ depends on this number, but how? The simplest way to answer this is to use dimensional analysis: $\tilde{\sigma}$, being itself dimensionless, may depend only on dimensionless variables. Therefore, it may depend on $p(E_c)$ only via the following dimensionless activation energy density: $\tilde{p} = p(E_c)/\beta$. As β diverges $\tilde{p} \to 0$ and we have universality: $\tilde{\sigma}$ becomes independent of both β and $p(E)$. The only assumptions needed for this argument to work are that $p(E)$ is smooth around E_c and that $p(E_c) > 0$. Note that, for finite β AC universality applies only in a finite range of frequencies which, however, broadens as $\beta \to \infty$. This is precisely what is observed in computer simulations (Fig. 5).

To understand AC universality for hopping we again refer to the equilibrium mean-square displacement. In terms of this quantity the frequency-dependent diffusion constant is given (Scher and Lax, 1973) by[12]

$$D(\omega) \;=\; -\frac{\omega^2}{2}\int_0^\infty \left\langle \Delta x^2(t)\right\rangle \; e^{-i\omega t}\; dt\,. \qquad (24)$$

We leave it to the reader to show that if the mean-square displacement is linear in time the diffusion constant is frequency-independent. At sufficiently long times the mean-square displacement indeed *is* linear in time, and consequently diffusion constant and conductivity are constant at sufficiently low frequencies.[13]

As shown already, when β is large the dominant contribution to the mean-square displacement comes from random walks on the fat percolation cluster. The links with smallest jump rate Γ_c on this cluster, the bottlenecks, determine the rate of mean-square displacement at long times which in turn determines the DC conductivity. The bottlenecks also determine the frequency marking onset of AC conduction, ω_m: Whenever $\Gamma_c t \gg 1$ many bottlenecks are passed in time t for a random walker on the fat percolation cluster; at these long times the mean-square displacement is linear in time. Consequently, conductivity is frequency-independent whenever $\omega \ll \Gamma_c$ (compare footnote 13). The mean-square displacement becomes

---

[12]Equation (24) is derived by two partial integrations of Eq. (16) utilizing the identity derived in footnote 10. An implicit convergence-factor $e^{-\epsilon t}$ ($\lim \epsilon \to 0$) is understood in the integral.

[13]For given ω the integral Eq. (24) is dominated by contributions to $\left\langle \Delta x^2(t)\right\rangle$ at times t given by $\omega t \sim 1$ (Tauberian theorem).

non-linear in time when $\Gamma_c t \sim 1$, corresponding to frequencies $\omega \sim \Gamma_c$, because then random walks on the cluster are limited to take place *between* bottlenecks. Thus, since both $\sigma(0)$ and ω_m are determined by Γ_c, we also for hopping arrive at the Barton-Nakajima-Namikawa rough proportionality Eq. (6).

From here on we argue much as for the macroscopic model. In a fixed range of times around the time above which the mean-square displacement is linear in time, corresponding to a fixed range of frequencies around ω_m, whenever β is large only links on the fat percolation cluster with activation energies close to E_c come into play as effective bottlenecks. $\tilde{\sigma}$ can depend only on $\tilde{p} = p(E_c)/\beta$ which goes to zero in the extreme disorder limit, thus establishing AC universality for the symmetric hopping model. Again, the only conditions for this to work are that $p(E)$ is smooth around E_c and that $p(E_c) > 0$.

The term "universality" became part of the physics vocabulary in the 1970's with the renormalization group theory of critical phenomena, one of the major advances in theoretical physics after World War II (Wilson, 1983; Goldenfeld, 1992). A second order phase transition is characterized by a number of critical exponents; universality refers to the fact that these depend only on dimension and order parameter symmetry, not on any microscopic details. In contrast, AC universality is not associated with exact power-laws. Despite this there is a connection to critical phenomena, because percolation *is* a critical phenomenon (see, e.g., Isichenko (1992)).

Approaching any second order phase transition there is a diverging correlation length. Is AC universality also associated with a diverging length? In our opinion the answer is yes. Consider first hopping and define l such that l^2 is the mean-square displacement at $t = 1/\omega_m$. It may be shown that in the effective medium approximation l diverges as $\beta \to \infty$. This is confirmed by our computer simulations. Presumably, l is the correlation length of the fat percolation cluster (Bouchaud and Georges, 1990). This identification makes it possible to define l for the macroscopic model as well and associate AC universality even for this model with a diverging correlation length.

The likely existence of a diverging characteristic length as $\beta \to \infty$ implies that AC universality is robust to rather extensive modifications of the two models, for instance by allowing resistors/jump rates which are not uncorrelated from link to link. As long as the resistors/jump rates have finite correlation length we expect that AC universality applies in the extreme disorder limit.

B. Percolation based approximations

To calculate the universal AC conductivity in either model the effective medium approximation introduces a homogeneous "effective medium." Although the effective medium approximation works well for the macroscopic model it is less successful for hopping. It may be possible to construct better approximations by making use of our knowledge that the current runs only on the fat percolation cluster. We shall do this in two tempi, each time developing an approximation applicable to both models.

The current running on the fat percolation cluster is not homogeneous. Computer simulations have shown that at extreme disorder the DC current follows almost one-dimensional paths (Brown and Esser, 1995). We now take a naive approach by regarding "conducting paths" as strictly one-dimensional. In the last section we saw that for both models most activation energies larger than E_c define links outside the fat percolation cluster, links which contribute little to the conductivity in the extreme disorder limit. Combining this fact with the assumption of strictly one-dimensional conducting paths, we arrive at the *percolation path approximation* (PPA): "The universal AC conductivity is the same as that of the extreme disorder limit of a one-dimensional model with sharp cut-off in the activation energy probability distribution."

It is easy to apply this approximation to the macroscopic model, because the one-dimensional analogue of Fig. 4 is exactly solvable. The macroscopic percolation path approximation for the universal AC conductivity thus found (Dyre, 1993) is:

$$\tilde{\sigma} = \frac{i\tilde{\omega}}{\ln(1+i\tilde{\omega})}. \qquad (25)$$

Compared to the solution of the effective medium approximation universality equation Eq. (13) this expression has a somewhat sharper onset of AC conduction (Fig. 10).

To apply the percolation path approximation to hopping, the AC conductivity in one dimension with a sharp activation energy cut-off must be calculated in the extreme disorder limit. This cannot be done analytically, the best one can do is to solve approximately. This was done by Dyre and Schrøder (1996) who showed that the effective medium approximation leads to the following equation (which accurately represents one-dimensional simulations)

$$\sqrt{\tilde{\sigma}}\,\ln\left(1+\sqrt{i\tilde{\omega}\,\tilde{\sigma}}\right) = \sqrt{i\tilde{\omega}}. \qquad (26)$$

Compared to the solution of the effective medium approximation universality equation this equation is somewhat less dramatic in the onset of AC conduction (Fig. 10).

We now proceed to develop a third approximation. The idea is the following. The effective medium approximation and the percolation path approximation are opposite extremes. The former views conduction as spatially homogeneous in an effective medium, the latter models conduction as one-dimensional. In reality, conduction takes place on a complex set we term the *diffusion cluster.*

How to define the diffusion cluster? Consider the DC limit. Not all links on the fat percolation cluster carry current - there are dead-ends. Removing these from the percolation cluster leaves us with the so-called "backbone" (Stauffer and Aharony, 1992). The backbone, which has dimension 1.7, contains loops however. This means that many pairs of sites are connected by two or more different paths on the backbone. In the extreme disorder limit one of these paths is by far most favorable. The backbone should therefore be further diluted by removing inefficient paths. A lower limit to this dilution is given by the set of so-called "red bonds," those with the property that if one of them is removed the backbone is broken into two parts. The set of red bonds has dimension 1.1. This set is not connected, however, so the diffusion cluster must be larger. We thus arrive at the following limits for the diffusion cluster dimension d_0:

$$1.1 < d_0 < 1.7. \tag{27}$$

To calculate $\tilde{\sigma}$ in the *diffusion cluster approximation* (DCA), the effective medium approximation is applied to conduction on the diffusion cluster. For the macroscopic model this leads straight to the effective medium approximation universality equation Eq. (13), which applies in the extreme disorder limit whenever $d_0 > 1$ (Dyre, 1993). For hopping the situation is different. When $d_0 < 2$ the hopping effective medium approximation does *not* lead to Eq. (13). Instead, the following expression is arrived at (Schrøder and Dyre, 1999)

$$\ln \tilde{\sigma} = \left(\frac{i\tilde{\omega}}{\tilde{\sigma}}\right)^{d_0/2}. \tag{28}$$

Figure 10 shows the solution of this equation for $d_0 = 1.35$, the value which best fit computer simulations (Schrøder and Dyre, 1999), together with the three other approximate analytical expressions for the two universal AC conductivities. All four expressions are summarized in Table I.

As mentioned already, the effective medium approximation works very well for the macroscopic model. Figure 11 compares the three approximations to hopping simulations, using a sensitive way to plot data by giving the apparent frequency-exponent n as function of $\tilde{\sigma}$. Clearly, the diffusion cluster approximation with $d_0 = 1.35$ gives a good representation of the numerical data. Remembering that for the macroscopic model the diffusion cluster approximation prediction is equal to that of the effective medium approximation which works very well (Eq. (13)), our conclusion is simple: For both models the diffusion cluster approximation works best.

VII. DISCUSSION

Before discussing model predictions and how they compare to experiment, let us briefly put our findings into a historical perspective. As mentioned in the Introduction, the full extent of AC universality was recognized in the 1970's. Already in the 1950's, however, it was discovered that the classical oxide glasses have more or less the same AC properties (Taylor 1956, 1957, 1959). At that time two models, predecessors to respectively the symmetric hopping model and the macroscopic model, were proposed: a) Stevels (1957) and Taylor (1956, 1959) assumed ions jump from one minimum to another in a random potential deriving from the random network structure of the glass (Zachariasen, 1932); b) Isard (1961) regarded the glass as a mixture of phases with different conductivity. Little progress was made with either model. Interestingly, it was for a long time believed that the time-temperature superposition principle implies that, if there is any activation energy distribution at all, it must be *narrow* compared to k_BT (Taylor, 1959; Owen, 1963; Isard, 1970). This belief was "confirmed" by two experimental facts: a) The DC conductivity is *not* non-Arrhenius as naively expected if a range of activation energies is involved; b) The DC conductivity is roughly proportional to the dielectric loss peak frequency (Eq. (6)), apparently implying that AC conduction is due to processes with same activation energy as DC conduction. This is all wrong. Ironically, we now know that AC universality - and thereby the time-temperature superposition principle - applies only when a range of activation energies *wide* compared to k_BT is involved. On the other hand, even though a broad range of activation energies contributes, in the extreme disorder limit everything *appears* to be controlled by just one activation energy, the E_c of Eq. (23) identified by percolation theory.

A. Model predictions

Let us compare the physics of the two models. The symmetric hopping model assumes disorder on a microscopic scale while the macroscopic model only assumes disorder on length scales large enough that the local conductivity concept makes sense. The symmetric hopping model ignores Coulomb repulsions between charge carriers, while the macroscopic model do take these fully into account via Maxwell's equations. The two models also differ in how external "control" enters: For hopping a spatially homogeneous externally electric field is assumed, while for the macroscopic model the field varies in space (in a way determined by the model itself) and only the potential difference across the sample is externally controlled. Despite these differences the models both predict AC universality in the extreme disorder limit and the two universal AC conductivities are similar.

Three approximations applicable to the universal AC conductivity of either model have been developed. Computer simulations show that for both models the best fit

is provided by the diffusion cluster approximation (for the macroscopic model the effective medium and the diffusion cluster approximations give same $\tilde{\sigma}(\tilde{\omega})$). The four analytical expressions (Fig. 10 and Table I) have the following crucial features in common: At low frequencies ($\tilde{\omega} \ll 1$) conductivity is frequency-independent, at high frequencies ($\tilde{\omega} \gg 1$) $\tilde{\sigma}'(\tilde{\omega})$ follows an approximate power-law with exponent $n < 1$. It can be shown that for all four expressions the frequency-exponent n is given by

$$\tilde{\omega} \to \infty : \; n \; = \; 1 \; - \; \frac{\alpha}{\ln \tilde{\omega}} . \qquad (29)$$

One finds $\alpha = 2$ for the effective medium approximation as well as for the macroscopic percolation path and diffusion cluster approximations. For the hopping percolation path approximation $\alpha = 3$, while the hopping diffusion cluster approximation has $\alpha = 1 + 2/d_0$. In all cases $n(\tilde{\omega}) \to 1$ for $\tilde{\omega} \to \infty$. This, in conjunction with the Barton-Nakajima-Namikawa relation's rough proportionality $\sigma(0) \sim \omega_m$,[14] is the key to explaining the 16 points summarizing the experimental findings in Section III. The details of proving this are left to the reader (Dyre, 1988).

We have focussed exclusively on the real part of the AC conductivity, but the imaginary part also becomes universal in the extreme disorder limit and follows an approximate power-law (with exponent close to n). There is however more to be said. It turns out (from effective medium calculations confirmed by computer simulations) that the convergence to universality for the imaginary part is slower than for the real part. In practice the imaginary part therefore contains more system-specific information than the real part.[15]

B. Models contra experiment

Figure 12 gives three examples comparing model predictions to experiment. First, Fig. 12(a) compares the very first published data indicating AC universality (Taylor, 1959) to our hopping model simulations in the extreme disorder limit. In this figure we follow Taylor by presenting dielectric loss as function of frequency. Figure 12(b) compares data for a several sodium-germanate glasses (Sidebottom, 1999) to the same hopping model simulations, again showing good agreement. Given the fact that the symmetric hopping model in the extreme disorder limit has no fitting parameters the fits in Figs. 12(a) and 12(b) are probably the best one can expect. Many similar data exist for ionic conductive glasses which are quite well fitted by the symmetric hopping model. Figure 12(c) presents AC data which are better fitted by the macroscopic model. These data are for a metal-cluster compound. It is generally believed that conduction in these solids, which proceeds via electrons tunneling between metal islands, is well described by the symmetric hopping model (van Staveren, Brom, and de Jongh, 1991). We find however that this is not so. The fact that the macroscopic model works better than hopping probably indicates that Coulomb interactions cannot be ignored for these systems.

C. Outlook

There are still many unsolved problems. Although one could argue (and we certainly do) that AC universality has been demonstrated beyond any reasonable doubt, no *rigorous* proof of AC universality in the extreme disorder limit exists for either model. Assuming AC universality, a number of problems remains:

- In regard to the diffusion cluster approximation - the one which works best for both models - it is important to precisely characterize the diffusion cluster and determine its dimension from analytical arguments and independent computer simulations.
- Both models have space elements (resistors/jump rates) with associated relaxation times much *longer* than the inverse loss peak frequency. These elements play little role for the magnitude of neither DC nor AC conductivity. One may however wonder whether they have other physical consequences, for instance by generating 1/f noise of the DC conductivity (Morozovskii and Snarskii, 1993).
- In any hopping model the complete characterization of random walks lies in the k-dependent frequency-dependent diffusion $D(k,\omega)$.[16] The obvious question now arises: Is $D(k,\omega)$ also universal

[14] Two of the four expressions in Table I (hopping percolation path and hopping diffusion cluster approximation) have no dielectric loss peaks and thus no loss peak frequency. This is an artifact of the approximations - in simulations both models do exhibit loss peaks. The relation $\omega_m \sim \sigma(0)$ however applies for all four approximations if ω_m is interpreted as the frequency marking onset of AC conduction.

[15] In principle the imaginary part is uniquely determined from the real part via the Kramers-Kronig relation (Landau and Lifshitz, 1969), but this requires that the real part is known at all frequencies.

[16] If $P(\mathbf{r},t)$ is the probability to find the charge carrier at site $\mathbf{r}$ at time t, given that it started at the origin at time 0, $D(k,\omega)$ is defined as follows: $1/(i\omega + k^2 D(k,\omega)) = \int_0^\infty dt\, e^{-i\omega t} \int d\mathbf{r} P(\mathbf{r},t) e^{i\mathbf{k}\cdot\mathbf{r}}$. For small k's $D(k,\omega)$ reduces to $D(\omega)$.

in the extreme disorder limit? If yes, for which k's is this the case?

- The symmetric hopping model arises when linearizing the hopping model with random site energies and Fermi-statistics (Shklovskii and Efros, 1984; Böttger and Bryksin, 1985), but how reliable is this linearization? In other words: Does this more realistic model exhibit AC universality in the extreme disorder limit and, if yes, does it have the same universal $\tilde{\sigma}(\tilde{\omega})$ as the hopping model?
- What about hopping models that are not symmetric: Do they exhibit AC universality always/sometimes/never?
- Does the disorder have to be static, as we have assumed throughout for both models, or can it be dynamic? For instance, would hopping on a *regular* lattice of charge carriers with Coulomb repulsions approach AC universality at low temperatures?

The above questions deal with the theoretical physics of AC universality. A main purpose however of future work should be to advance our understanding to the point where reliable information about conduction mechanisms can be obtained from AC data and their *deviations* from universality. It seems to us that we are only at the beginning of such endeavors.

ACKNOWLEDGMENTS

This paper is based on talks given by JCD in Leipzig and Marburg (Germany) in May 1999. Friedrich Kremer and Sergei Baranovskii are thanked for their most kind hospitality in hosting these visits.

REFERENCES

Alexander, S., J. Bernasconi, W. R. Schneider, and R. Orbach, 1981, Rev. Mod. Phys. **53**, 175.
Ambegaokar, V., B. I. Halperin, and J. S. Langer, 1971, Phys. Rev. B **4**, 2612.
Angell, C. A., 1990, Chem. Rev. **90**, 523.
Balkan, N., P. N. Butcher, W. R. Hogg, A. R. Long, and S. Summerfield, 1985, Philos. Mag. B **51**, L7.
Barton, J. L., 1966, Verres et Refr. **20**, 328.
Becker, R., 1967, *Theory of Heat* (Springer, Berlin).
Berryman, J. G., 1980, J. Acoust. Soc. Am. **68**, 1820.
Bianchi, R. F., P. H. Souza, T. J. Bonagamba, H. C. Panepucci, and R. M. Faria, 1999, Synthetic Metals **102**, 1186.
Böttcher, C. J. F., and P. Bordewijk, 1978, *Theory of Electric Polarization*, Vol. 2 (Elsevier, Amsterdam).
Böttger, H., and V. V. Bryksin, 1985, *Hopping Conduction in Solids* (Akademie, Berlin).
Bouchaud, J.-P., and A. Georges, 1990, Phys. Rep. **195**, 127.
Broadbent, S. R., and J. M. Hammersley, 1957, Proc. Camb. Phil. Soc. **53**, 629.
Brown, R., and B. Esser, 1995, Philos. Mag. B **72**, 125.
Bruggeman, D. A. G., 1935, Ann. Phys. (Leipzig) **24**, 636.
Bryksin, V. V., 1980, Fiz. Tverd. Tela (Leningrad) **22**, 2441 [Sov. Phys. Solid State **22**, 1421].
Durand, B., G. Taillades, A. Pradel, M. Ribes, J. C. Badot, and N. Belhadj-Tahar, 1994, J. Non-Cryst. Solids **172-174**, 1306.
Dyre, J. C., 1988, J. Appl. Phys. **64**, 2456.
Dyre, J. C., 1993, Phys. Rev. B **48**, 12511.
Dyre, J. C., 1994, Phys. Rev. B **49**, 11709; **50**, 9692 (E).
Dyre, J. C., and J. M. Jacobsen, 1995, Phys. Rev. E **52**, 2429.
Dyre, J. C., and T. B. Schrøder, 1996, Phys. Rev. B **54**, 14884.
Elliott, S. R., 1990, *Physics of Amorphous Materials*, 2nd ed. (Longman Scientific, London).
Elliott, S. R., 1994, Solid State Ionics **70/71**, 27.
Economou, E. N., 1983, *Green's Functions in Quantum Physics*, 2nd edition (Springer, Berlin).
Epstein, A. J., 1986, in *Handbook of Conjugated Electrically Conducting Polymers*, edited by T. A. Skotheim (Marcel Dekker, New York, 1986), Vol. 2, p. 1041.
Fiegl, B., R. Kuhnert, M. Ben-Chorin, and F. Koch, 1994, Appl. Phys. Lett. **65**, 371.
Fishchuk, I. I., 1986, Phys. Status Solidi A **93**, 675.
Funke, K., 1993, Prog. Solid State Chem. **22**, 111.
Ghosh, A., and M. Sural, 1999, Europhys. Lett. **47**, 688.
Goldenfeld, N., 1992, *Lectures on Phase Transitions and the Renormalization Group* (Addison-Wesley, Reading, Massachusetts).
Haus, J. W., and K. W. Kehr, 1987, Phys. Rep. **150**, 263.
Howell, F. S., R. A. Bose, P. B. Macedo, and C. T. Moynihan, 1974, J. Phys. Chem. **78**, 639.
Hughes, B. D., 1996, *Random Walks and Random Environments*, Vol. 2 (Clarendon, Oxford).
Hunt, A., 1995, J. Non-Cryst. Solids **183**, 109.
Isard, J. O., 1961, Proc. Inst. Elec. Eng. **109B**, Suppl. No. 22, 440 [The Institution of Electrical Engineers, Paper No. 3636].
Isard, J. O., 1970, J. Non-Cryst. Solids **4**, 357.
Isichenko, M. B., 1992, Rev. Mod. Phys. **64**, 961.
Jastrzebska, M. M., S. Jussila, and H. Isotalo, 1998, J. Mater. Sci. **33**, 4023.
Jonscher, A. K., 1977, Nature **267**, 673.
Jonscher, A. K., 1996, *Universal Relaxation Law* (Chelsea Dielectric, London).
Kahnt, H., 1991, Ber. Bunsenges. Phys. Chem. **95**, 1021.
Kimball, J. C., and L. W. Adams, Jr., 1978, Phys. Rev. B **18**, 5851.
Kirkpatrick, S., 1973, Rev. Mod. Phys. **45**, 574.
Kittel, C., 1996, *Introduction to Solid State Physics*, seventh edition (John Wiley & Sons, New York).
Kremer, F., 1999, personal communication.
Kuanr, B. K., and G. P. Srivastava, 1994, J. Appl. Phys. **75**, 6115.
Kubo, R., 1957, J. Phys. Soc. Jpn. **12**, 570.
Kulkarni, A. R., P. Lunkenheimer, and A. Loidl, 1998, Solid State Ionics **112**, 69.
Lakatos, A. I., and M. Abkowitz, 1971, Phys. Rev. B **3**, 1791.

Landau, L. D., and E. M. Lifshitz, 1969, *Statistical Physics* 2nd edition (Pergamon, Oxford).
Lidiard, A. B., 1957, in *Handbuch der Physik*, edited by S. Flügge, Vol. 20, p. 246.
Lim, B. S., A. V. Vaysleyb, and A. S. Nowick, 1993, Appl. Phys. A **56**, 8.
Long, A. R., and N. B. Balkan, 1980, J. Non-Cryst. Solids **35-36**, 415.
Long, A. R., 1982, Adv. Phys. **31**, 553.
Macdonald, J. R., 1997, J. Non-Cryst. Solids **210**, 70.
Mansingh, A., 1980, Bull. Mater. Sci. (India) **2**, 325.
Maxwell, J. C., 1891, *A Treatise of Electricity and Magnetism*, Vol. 1 (Clarendon, Oxford).
Miller, A., and B. Abrahams, 1960, Phys. Rev. **120**, 745.
Morozovskii, A. E., and A. A. Snarskii, 1993, Zh. Eksp. Teor. Fiz. **104**, 4059 [Sov. Phys. JETP **77**, 959].
Mott, N. F., and E. A. Davis, 1979, *Electronic Processes in Non-crystalline Materials*, 2nd ed. (Clarendon, Oxford).
Nakajima, T., 1972, in *Conference on Electrical Insulation and Dielectric Phenomena* (National Academy of Sciences, Washington, DC), p. 168.
Namikawa, H., 1975, J. Non-Cryst. Solids **18**, 173.
Ngai, K. L., and C. T. Moynihan, 1998, MRS Bulletin **23**, 51.
Owen, A. E., 1963, in *Progress in Ceramic Science*, edited by J. E. Burke (Macmillan, New York), Vol. 3, p. 77.
Owen, A. E., 1977, J. Non-Cryst. Solids **25**, 370.
Pollak, M., and T. H. Geballe, 1961, Phys. Rev. **122**, 1742.
Reedijk, J. A., L. J. Adriaanse, H. B. Brom, L. J. de Jongh, and G. Schmid, 1998, Phys. Rev. B **57**, R15116.
Rehwald, W., H. Kiess, and B. Binggeli, 1987, Z. Phys. B **68**, 143.
Reitz, J. R., F. J. Milford, and R. W. Christy, 1993, *Foundations of Electromagnetic Theory*, fourth edition (Addison-Wesley, Reading, Massachusetts).
Riedel, T., and J. C. Dyre, 1994, J. Non-Cryst. Solids **172-174**, 1419.
Roling, B., A. Happe, K. Funke, and M. D. Ingram, 1997, Phys. Rev. Lett. **78**, 2160.
Roling, B., 1998, Solid State Ionics **105**, 185.
Rozanski, S. A., F. Kremer, P. Köberle, and A. Laschewsky, 1995, Macromol. Chem. Phys. **196**, 877.
Russell, B., 1946, *A history of western philosophy* (George Allen and Unwin Ltd, London).
Scher, H., and M. Lax, 1973, Phys. Rev. B **7**, 4491 and 4502.
Schrøder, T. B., 1999, Ph.D. thesis (Roskilde University).
Schrøder, T. B., and J. C. Dyre, 1999, Phys. Rev. Lett. (in press).
Shklovskii, B. I., and A. L. Efros, 1971, Zh. Eksp. Teor. Fiz. **60**, 867 [Sov. Phys. JETP **33**, 468].
Shklovskii, B. I., and A. L. Efros, 1984, *Electronic Properties of Doped Semiconductors* (Springer, Berlin).
Sidebottom, D. L., 1999, Phys. Rev. Lett. **82**, 3653.
Stauffer, D., and A. Aharony, 1992, *Introduction to Percolation Theory*, 2nd ed. (Taylor and Francis, London).
Stein, D. L., and C. M. Newman, Phys. Rev. E, 1995, **51**, 5228.
Stevels, J. M., 1957, in *Handbuch der Physik*, edited by S. Flügge, Vol. 20, p. 350.
Summerfield, S., 1985, Philos. Mag. B **52**, 9.
Suzuki, M., 1980, J. Phys. Chem. Solids **41**, 1253.
Taylor, H. E., 1956, Trans. Faraday Soc. **52**, 873.
Taylor, H. E., 1957, J. Soc. Glass Tech. **41**, 350T.
Taylor, H. E., 1959, J. Soc. Glass Tech. **43**, 124T.
Tyč, S., and B. I. Halperin, 1989, Phys. Rev. B **39**, 877.
van Heumen, J., W. Wieczorek, M. Siekierski, and J. R. Stevens, 1995, J. Phys. Chem. **99**, 15142.
van Kampen, N. G., 1981, *Stochastic processes in physics and chemistry* (North-Holland, Amsterdam).
van Staveren, M. P. J., H. B. Brom, and L. J. de Jongh, 1991, Phys. Rep. **208**, 1.
Wagner, K. W., 1913, Ann. Phys. (Leipzig) **40**, 817.
Wilson, K. G., 1983, Rev. Mod. Phys. **55**, 583.
Wolynes, P. G., 1992, Acc. Chem. Res. **25**, 513.
Zachariasen, W. H., 1932, J. Am. Chem. Soc. **54**, 3841.
Ziman, J. M., 1979, *Models of disorder* (Cambridge University, Cambridge).

FIG. 1. Experimental AC universality. AC conductivity of typical ionically (a-c) and electronically (d-f) conducting disordered solids. Each figure shows a log-log plot of the real part of the conductivity as function of frequency at various temperatures. At low frequencies the conductivity is constant, at high frequencies the conductivity follows an approximate power-law with exponent below one. (a) $50LiF - 30KF - 20Al(PO_3)_3$ glass (inset: real part of dielectric constant) (Kulkarni, Lunkenheimer, and Loidl, 1998); (b) $0.4Ca(NO_3)_2 - 0.6KNO_3$ extremely viscous liquid (Howell *et al.*, 1974); (c) Thermoplastic polyurethane doped with $NH_4CF_3SO_3$ (van Heumen *et al.*, 1995); (d) Poly(methylthiophene) (Rehwald, Kiess, and Binggeli, 1987); (e) Amorphous germanium film (inset: frequency-exponent as function of temperature) (Long and Balkan, 1980); (f) Polycrystalline diamond film (Fiegl *et al.*, 1994).

FIG. 2. AC conductivity master curves. Each figure shows a log-log plot the real part of the quantity $\tilde{\sigma}$ defined in Eq. (3) as function of a scaled frequency. (a) gives the master curve for the ionic conductive glass data of Fig. 1(a) (Kulkarni, Lunkenheimer, and Loidl, 1998); (b) gives the master curve for the electronic conducting polymer data of Fig. 1(d) (Rehwald, Kiess, and Binggeli, 1987); (c) gives the common master curve for data on eight different ionic conductive glasses (Roling, 1998).

FIG. 3. Barton-Nakajima-Namikawa relation (Eq. (5)) for 40 different alkali ion conducting glasses. The broken line corresponds to $p = 1$ in Eq. (5). These data from four different laboratories were compiled by Nakajima (1972) who presented a similar figure for 14 electronically conducting transition metal oxide glasses.

FIG. 4. Electrical equivalent circuit arising from discretizing Maxwell's equations for an inhomogeneous conductor. This circuit describes the macroscopic model (Fishchuk, 1986; Dyre, 1993). All capacitors are equal, proportional to ϵ_∞, while each resistor is proportional to $\exp(\beta E)$ where $\beta = 1/k_BT$ and E is the random activation energy. In an external (DC or AC) field the electrostatic potentials at the nodes are found from Kirchhoff's equations. The resistor currents are the free charge currents. The capacitor currents are Maxwell's displacement currents, parts of which are bound charge currents and parts of which are "ghost" currents. Thus in AC fields bound and free charge may accumulate at nodes without violating Kirchhoff's laws.

FIG. 5. Computer simulations of the macroscopic model in two dimensions (reproduced from Dyre (1993)). (a) shows $\tilde{\sigma}$ as function of scaled *imaginary* frequency (scaling defined in Dyre (1993)) for the activation energy probability distribution $p(E) = 2E\,(0 \leq E \leq 1)$ at β equal to 5, 10, 20, 40, 80, 160 in order of increasing conductivity. The full curves are the predictions of the effective medium approximation. (b) shows results for six different activation energy probability distributions at β=160 in two dimensions compared to the effective medium approximation universality equation (13). At extreme disorder all distributions have same "universal" $\tilde{\sigma}$ which is well represented by the effective medium approximation universality equation (13).

FIG. 6. Typical potential felt by a charge carrier in one dimension described by the symmetric hopping model. The symmetric hopping model corresponds to the discrete version of motion in this potential, where charge carriers reside on a lattice (the minima), making instantaneous jumps over the barriers connecting nearest neighbor sites. At temperatures low compared to the barriers most time is spent close to energy minima. Occasionally, the charge carrier by chance acquires enough energy from the surrounding heat bath to jump into a neighboring minimum. If the barrier height is E, the probability of this happening per unit time is proportional to $\exp(-\beta E)$ ($\beta = 1/k_BT$). At low temperatures the charge carrier almost always chooses the lowest barrier, leading to the "bounce-back effect:" After one jump the next jump most likely goes back again (Kimball and Adams, 1978).

FIG. 7. (a) Mean-square displacement and (b) velocity auto-correlation function as function of time for a charge carrier in the symmetric hopping model. In the homogeneous case with only one jump rate, the mean-square displacement is linear in time and the velocity auto-correlation function is a delta-function at $t = 0$ and zero whenever $t > 0$. In the inhomogeneous case, as shown in the text and Fig. 6, after one jump the next usually goes back again. This "bounce-back effect" causes the mean-square displacement to be faster at short times than expected from an extrapolation of the long-time (linear) limit (Kimball and Adams, 1978; Funke, 1993). The velocity auto-correlation function, being the second time-derivative of the mean-square displacement (footnote 10), is consequently negative for $t > 0$, and only positive right at $t = 0$ where it is a delta-function.

FIG. 8. Computer simulations of the symmetric hopping model in three dimensions. (a) Real part of the AC conductivity in "rationalized units" for the Box distribution of activation energies ($p(E) = 1$, $0 \leq E \leq 1$) at four different inverse temperatures; (b) the same data scaled according to Eq. (7), clearly showing convergence to one single curve as $\beta \to \infty$; (c) data for five different activation energy probability distributions at large β's, showing universality, i.e., that the AC conductivity at extreme disorder is independent of probability distribution. The full curve is the prediction of the effective medium approximation (EMA) universality equation (13), also scaled according to Eq. (7). The simulations were carried out by solving the hopping master equation using a new numerically stable algorithm (Schrøder, 1999). The figures (b) and (c) are reproduced from Schrøder and Dyre (1999).

FIG. 9. Percolation in two dimensions. On an underlying square lattice (not shown) each link is marked black with probability p. (a) If p is below the so-called percolation threshold p_c no connected cluster exists extending to infinity; (b) if $p > p_c$ there is such a cluster. The percolation threshold is precisely 0.5 in two dimensions and approximately 0.25 in three dimensions (Isichenko, 1992). As argued in the text, the percolation phenomenon is central to understanding AC universality for both models.

FIG. 10. Comparison of the real part of the four approximate analytical expressions for the universal AC conductivities of the two models (Table I) derived in: the effective medium approximation (EMA), the percolation path approximation (PPA), the diffusion cluster approximation (DCA). The frequency scaling is here defined such that all four curves coincide at $\log_{10}(\tilde{\sigma}') = 0.5$. As a guide to the eye, dots are shown marking a line with slope one. All four expressions follow an approximate power-law at high frequencies with exponent below one which converges to one as scaled frequency goes to infinity.

FIG. 11. The apparent exponent $n \equiv d\ln\tilde{\sigma}'/d\ln\tilde{\omega}$ plotted as function of $\tilde{\sigma}'$ for the universal AC conductivity found from simulations of the symmetric hopping model (symbols as in Fig. 8(c)). The predictions of the three analytical approximations (EMA, PPA, DCA) are shown as curves. The numerical data are best fitted by the diffusion cluster approximation with $d_0 = 1.35$.

FIG. 12. Models compared to experiment. (a) gives the dielectric loss (negative imaginary part of $\epsilon(\omega)$ defined in Eq. (2)) for the first data published showing AC universality (full symbols, data for five different ionic conductive oxide glasses taken from Fig. 5 in Taylor (1959)) compared to our simulations of the symmetric hopping model in the extreme disorder limit (open symbols as in Fig. 8(c)). The high-frequency experimental data-points were obtained by extrapolation, assuming time-temperature superposition (Taylor, 1959). (b) shows the $\tilde{\sigma}'$-data of Sidebottom (1999) on sodium-germanate glasses compared to our symmetric hopping model simulations in the extreme disorder limit, both data sets scaled according to Eq. (7). Also shown are the hopping diffusion cluster approximation (DCA, representing hopping) and the macroscopic diffusion cluster approximation (DCA = EMA, representing the macroscopic model) (reproduced from Schrøder and Dyre (1999)); (c) shows data for the metal cluster compound Pd-7/8 (Reedijk *et al.*, 1998) compared to our symmetric hopping model simulations. Also shown are the hopping diffusion cluster approximation (DCA, representing hopping) and the macroscopic diffusion cluster approximation (DCA = EMA, representing the macroscopic model). In this figure the frequency scaling was fixed by requiring same $\tilde{\sigma}'$ at the highest frequencies for data as well as for the two analytical approximations.

TABLE I. AC Universality equations.

	Macroscopic model	Symmetric hopping model
Effective medium approximation[a]	$\tilde{\sigma}\ \ln\tilde{\sigma} = i\tilde{\omega}$	$\tilde{\sigma}\ \ln\tilde{\sigma} = i\tilde{\omega}$
Percolation path approximation[b]	$\tilde{\sigma} = \frac{i\tilde{\omega}}{\ln(1+i\tilde{\omega})}$	$\sqrt{\tilde{\sigma}}\ln\left(1+\sqrt{i\tilde{\omega}\tilde{\sigma}}\right) = \sqrt{i\tilde{\omega}}$
Diffusion cluster approximation[c]	$\tilde{\sigma}\ \ln\tilde{\sigma} = i\tilde{\omega}$	$\ln\tilde{\sigma} = \left(\frac{i\tilde{\omega}}{\tilde{\sigma}}\right)^{d_0/2}$

[a]Equation (13).
[b]Equations (25) and (26).
[c]Equations (13) and (28).

Fig. 1

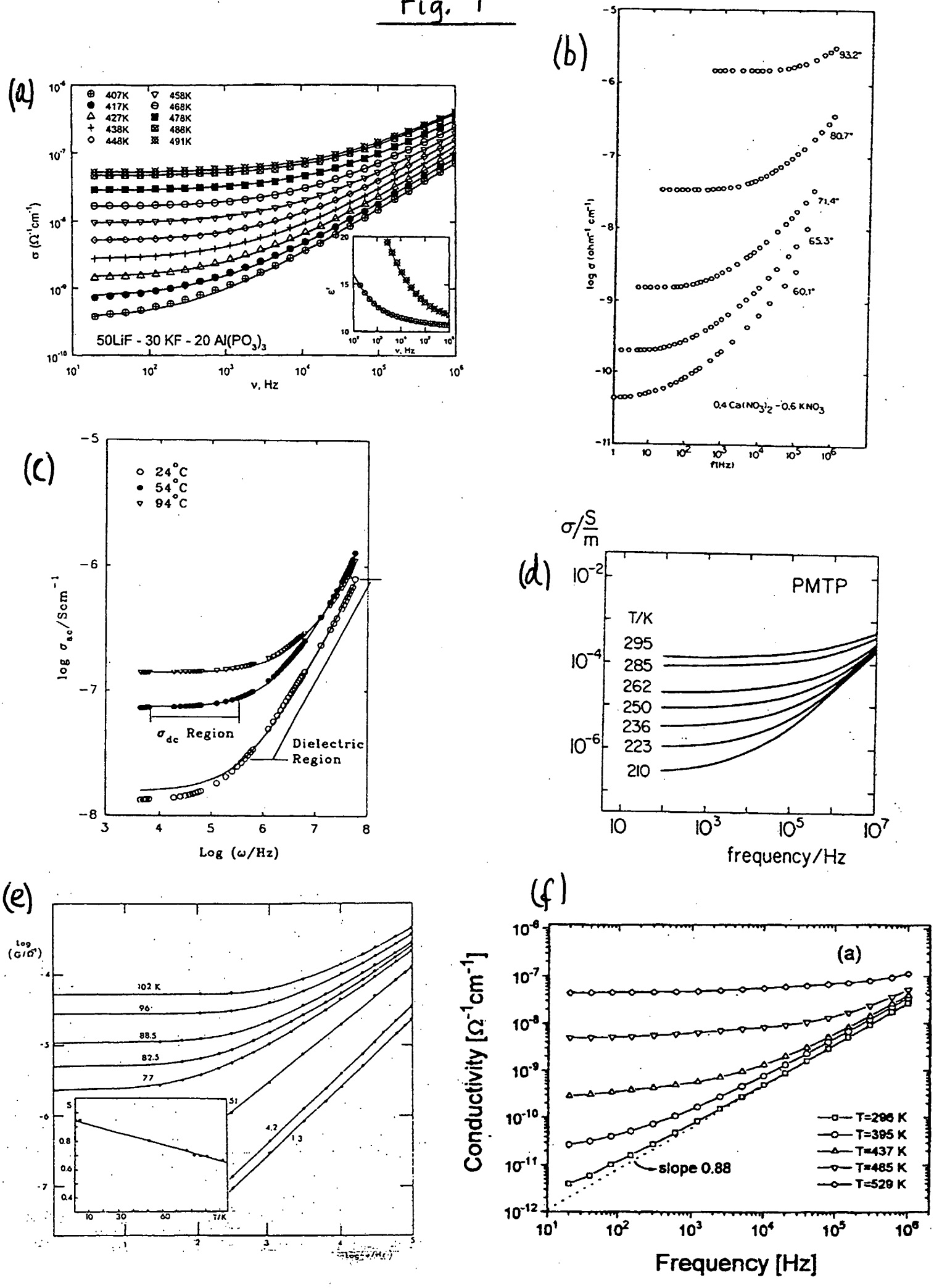
(a)
407K
417K
427K
438K
448K
458K
468K
478K
488K
491K
σ (Ω⁻¹cm⁻¹)
50LiF - 30 KF - 20 Al(PO3)3
ν, Hz
ε'
ν, Hz
(b)
93.2°
80.7°
71.4°
65.3°
60.1°
log σ (ohm⁻¹ cm⁻¹)
0.4 Ca(NO3)2 - 0.6 KNO3
f(Hz)
(c)
24°C
54°C
94°C
log σac/Scm⁻¹
σdc Region
Dielectric Region
Log (ω/Hz)
(d)
σ/S/m
PMTP
T/K
295
285
262
250
236
223
210
frequency/Hz
(e)
Log (G/Ω⁻¹)
102 K
96
88.5
82.5
77
51
4.2
1.3
T/K
(f)
Conductivity [Ω⁻¹cm⁻¹]
(a)
T=296 K
T=395 K
T=437 K
T=485 K
T=529 K
slope 0.88
Frequency [Hz]

Fig. 2

(a)

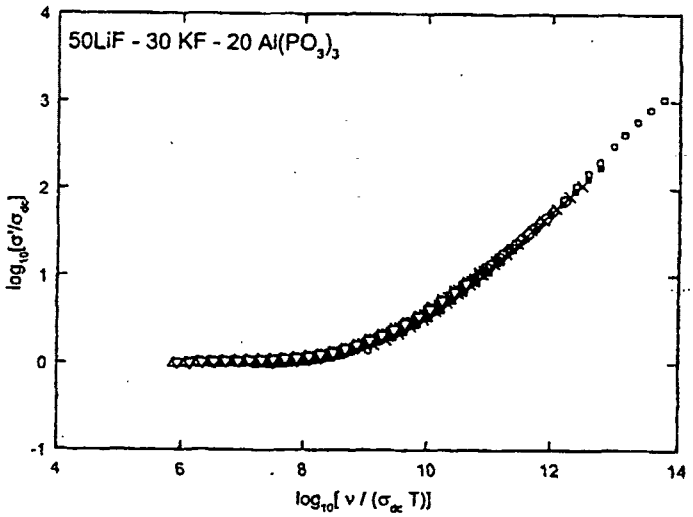
50LiF - 30 KF - 20 Al(PO3)3
log10[σ'/σdc]
log10[ν / (σdc T)]

(b)

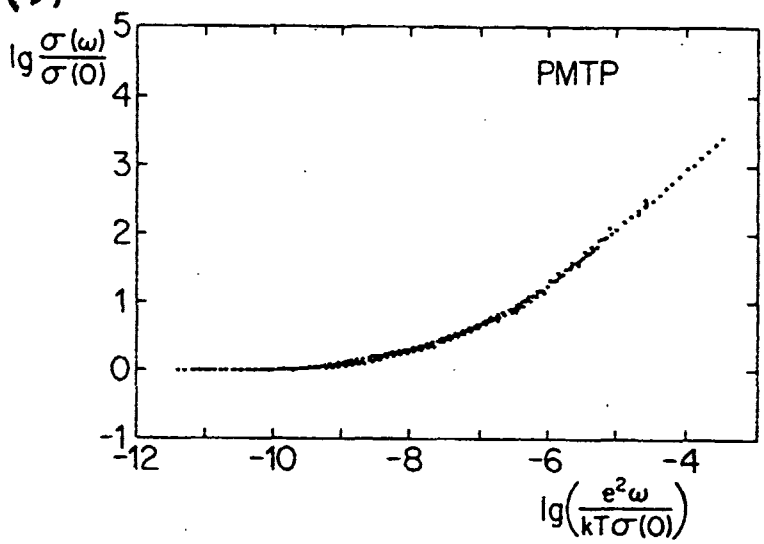
lg σ(ω)/σ(0)
PMTP
lg(e²ω/kTσ(0))

(c)

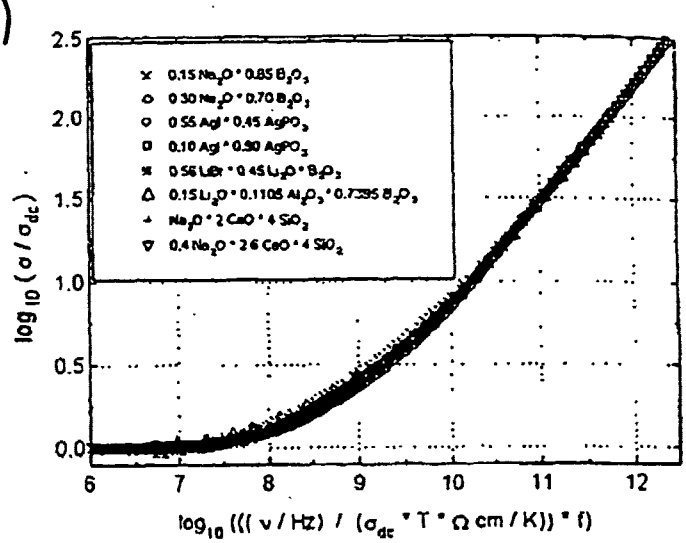
0.15 Na2O * 0.85 B2O3
0.30 Na2O * 0.70 B2O3
0.55 AgI * 0.45 AgPO3
0.10 AgI * 0.90 AgPO3
0.56 LiBr * 0.44 Li2O * B2O3
0.15 Li2O * 0.1105 Al2O3 * 0.7395 B2O3
Na2O * 2 CaO * 4 SiO2
0.4 Na2O * 2.6 CaO * 4 SiO2
log10 (σ / σdc)
log10 (((ν / Hz) / (σdc * T * Ω cm / K)) * f)

Fig. 3

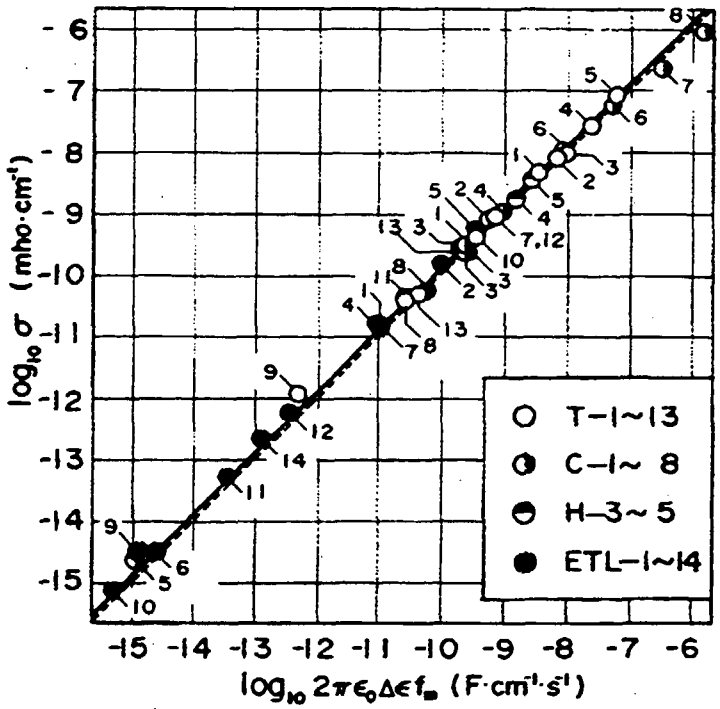
- 6
- 7
- 8
- 9
-10
-11
-12
-13
-14
-15
$\log_{10}\sigma$ (mho·cm^{-1})
-15 -14 -13 -12 -11 -10 -9 -8 -7 -6
$\log_{10} 2\pi\epsilon_0\Delta\epsilon f_m$ (F·cm^{-1}·s^{-1})
T-1~13
C-1~ 8
H-3~ 5
ETL-1~14

Fig. 4

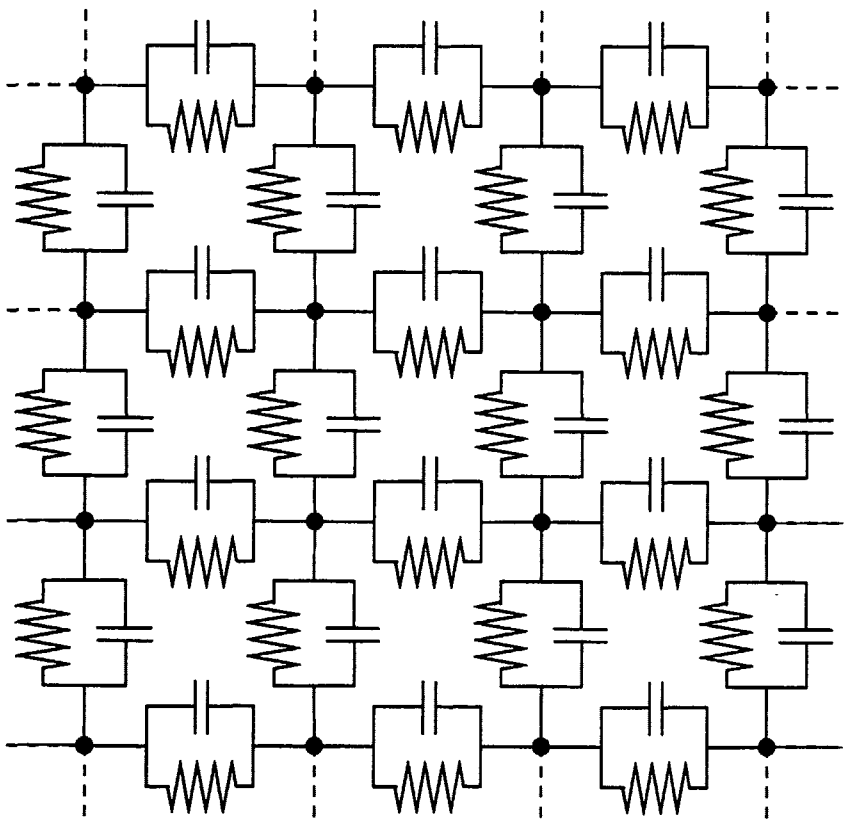

Fig. 5(a)

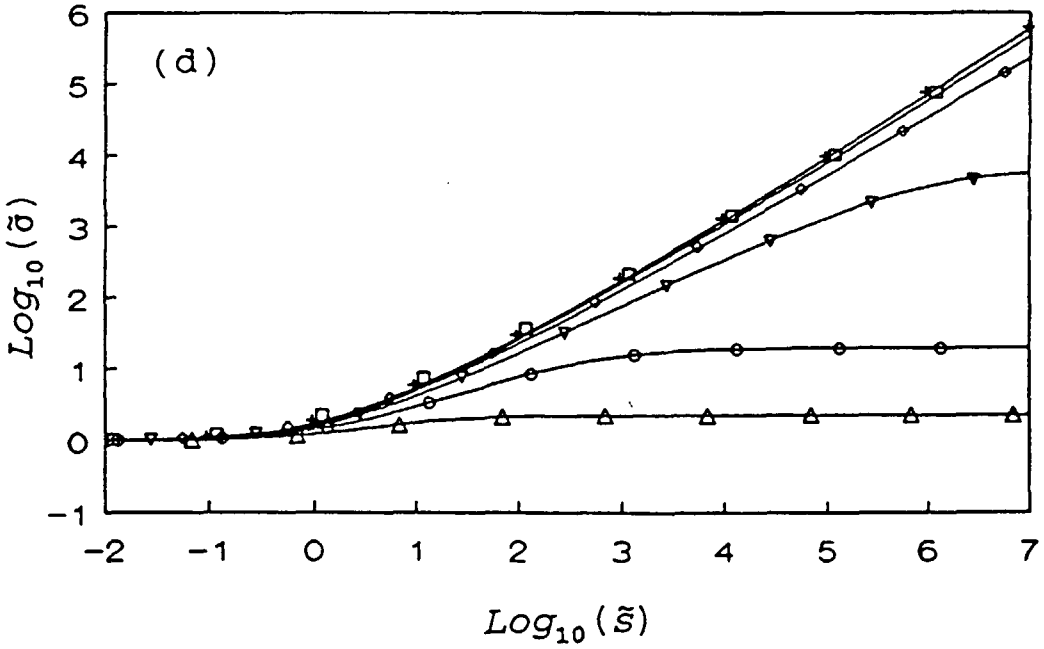

Fig. 5 (b)

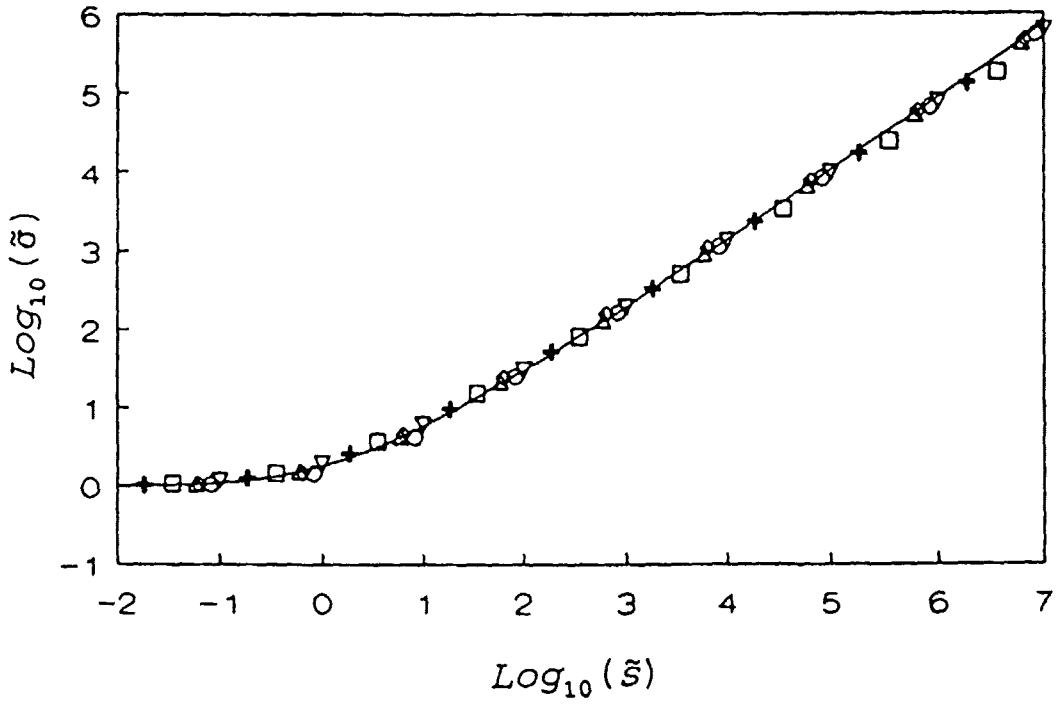

Fig. 6

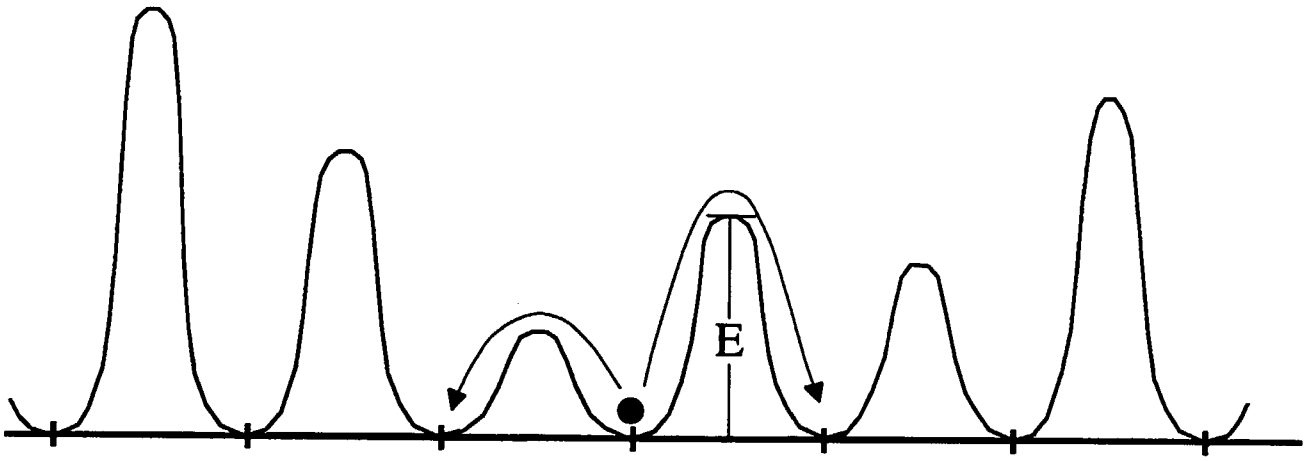

Fig. 7(a)

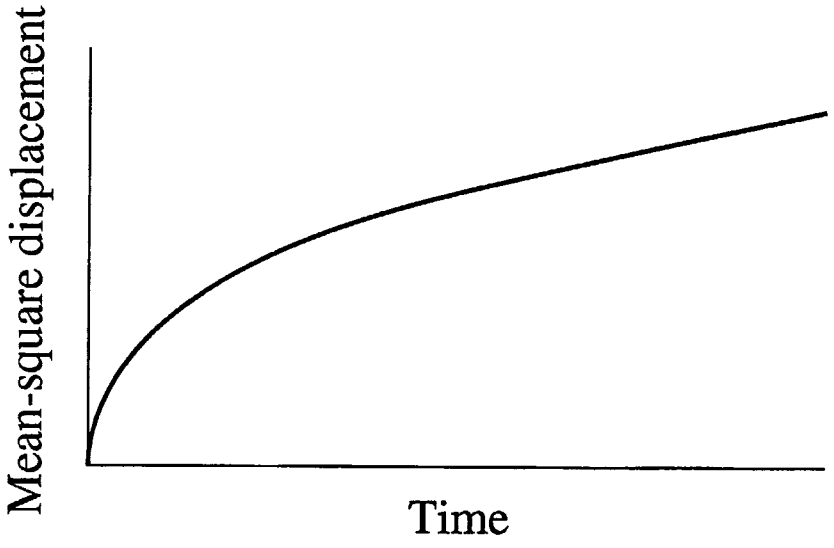

Fig. 7(b)

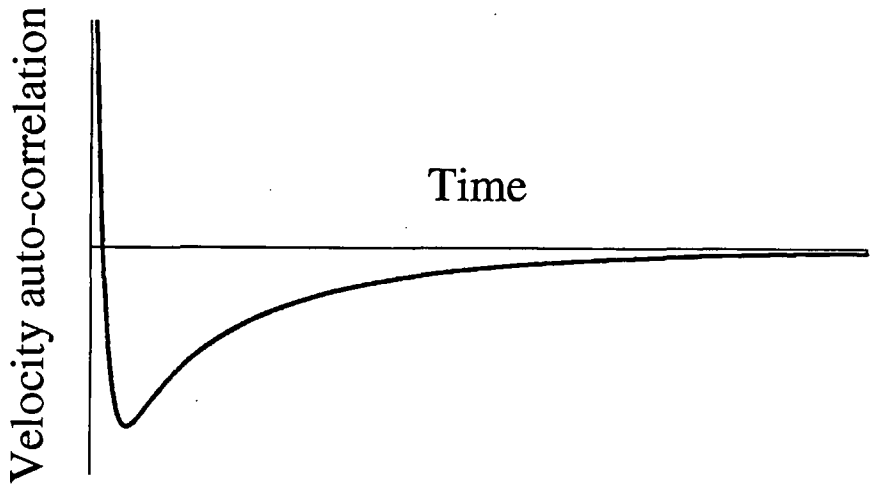

Fig. 8 (a)

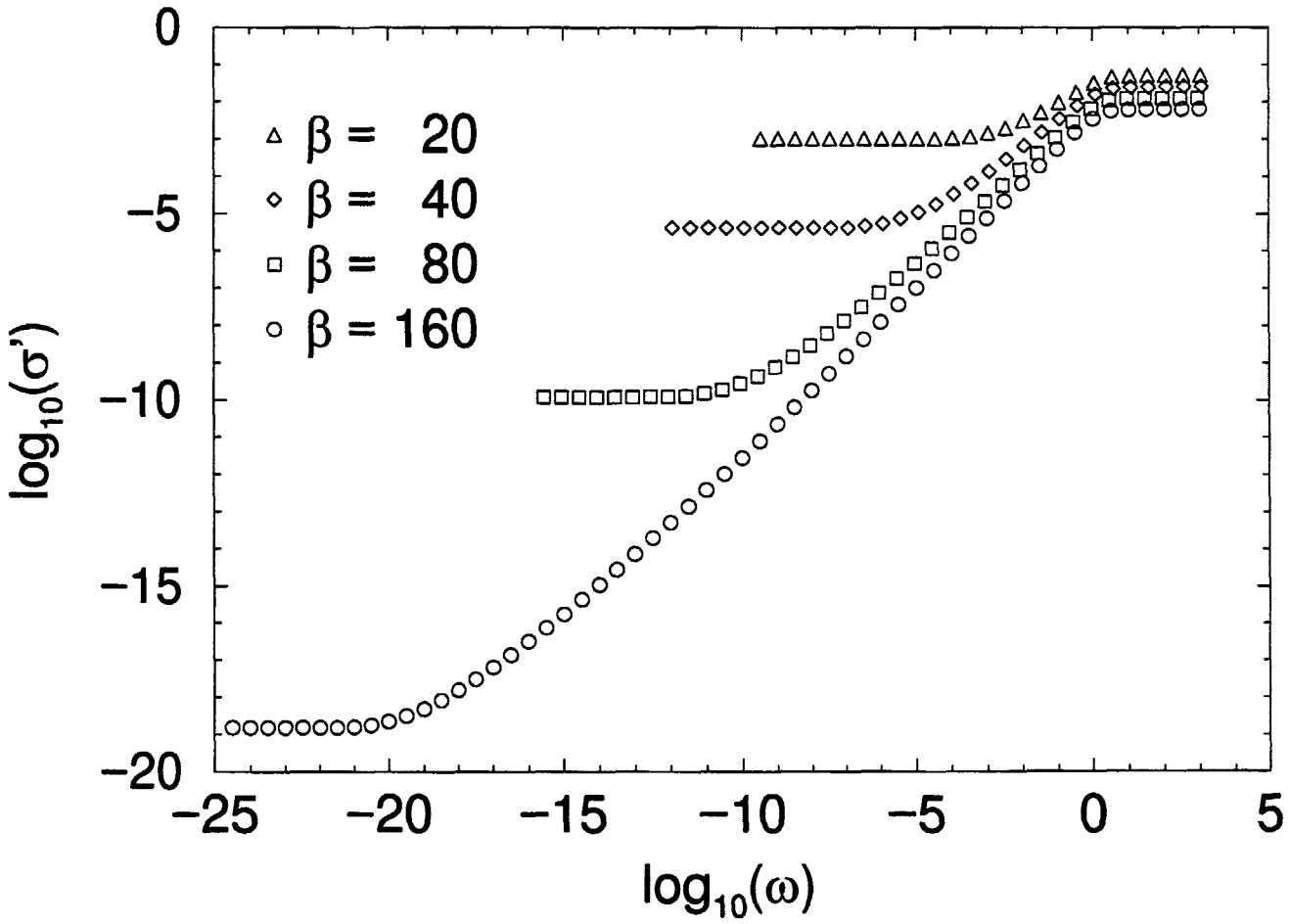

Fig. 8(b)

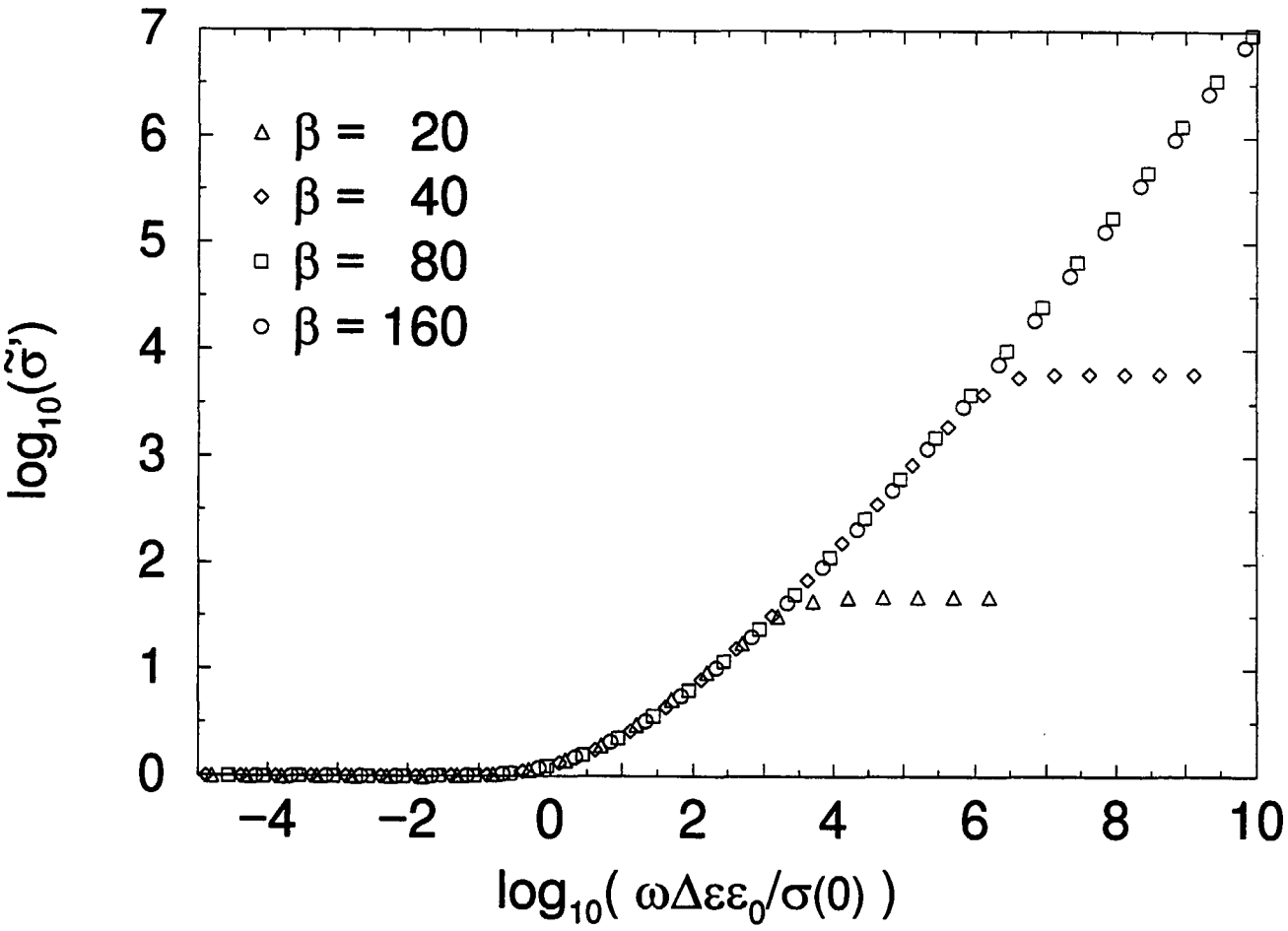

Fig. 8(c)

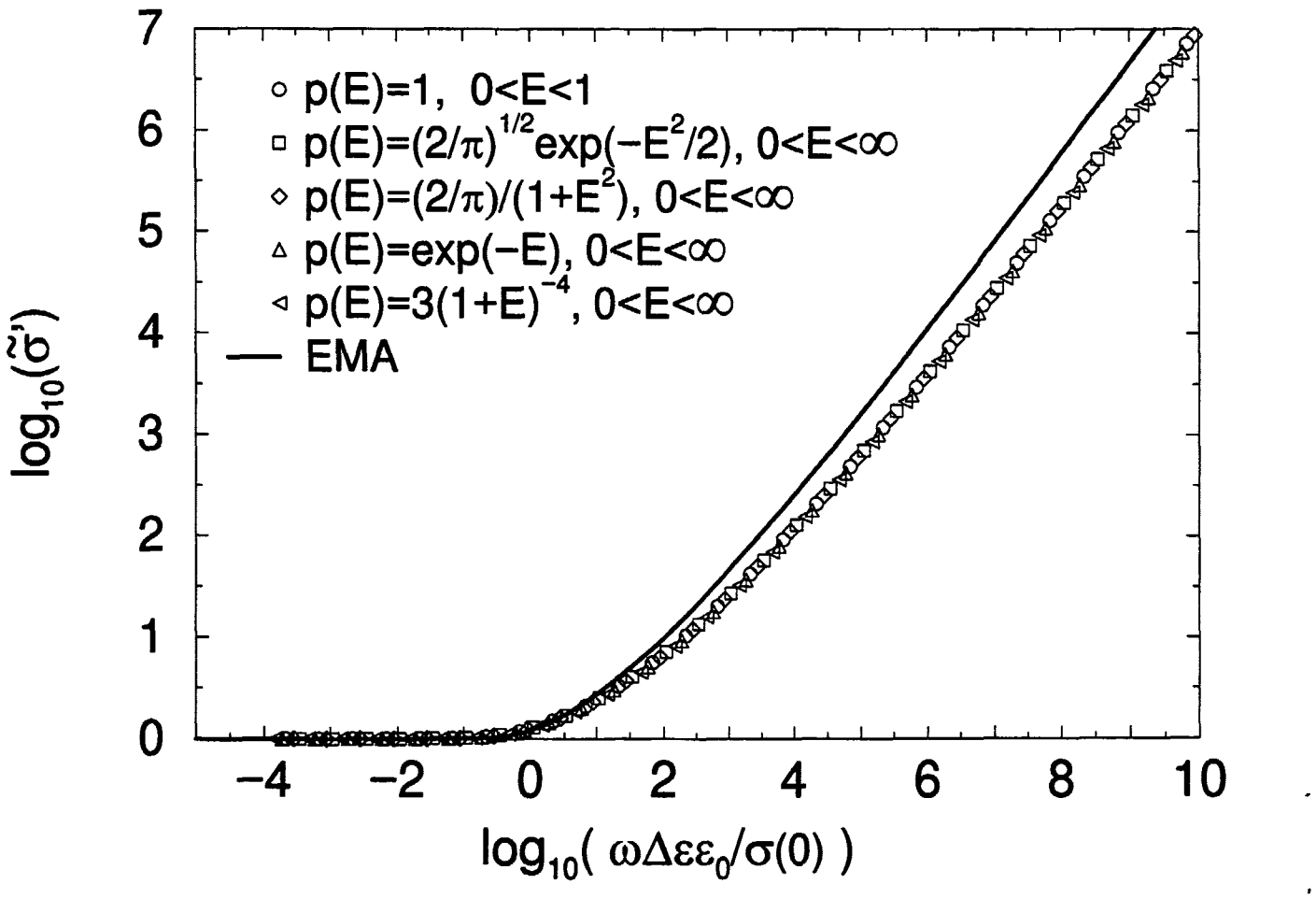
p(E)=1, 0<E<1
p(E)=(2/π)^1/2 exp(−E^2/2), 0<E<∞
p(E)=(2/π)/(1+E^2), 0<E<∞
p(E)=exp(−E), 0<E<∞
p(E)=3(1+E)^−4, 0<E<∞
EMA
log10(σ̃')
log10(ωΔεε0/σ(0))
0
1
2
3
4
5
6
7
−4
−2
0
2
4
6
8
10

Fig. 9(a)

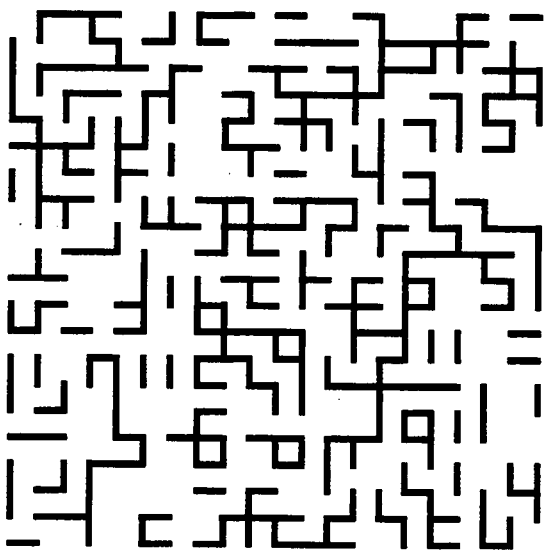

$p < p_c$

Fig. 9(b)

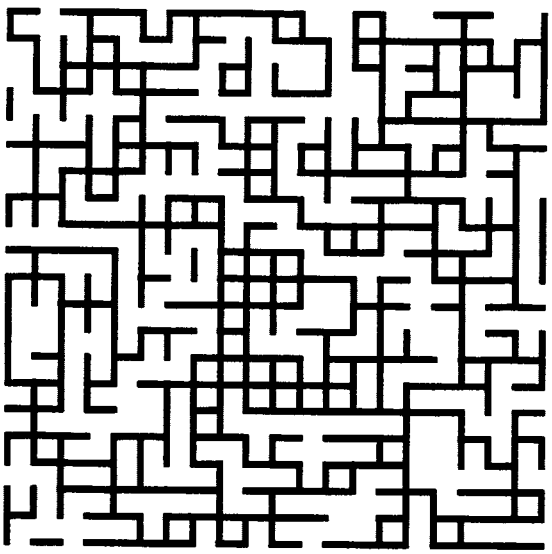

$p > p_c$

Fig. 10

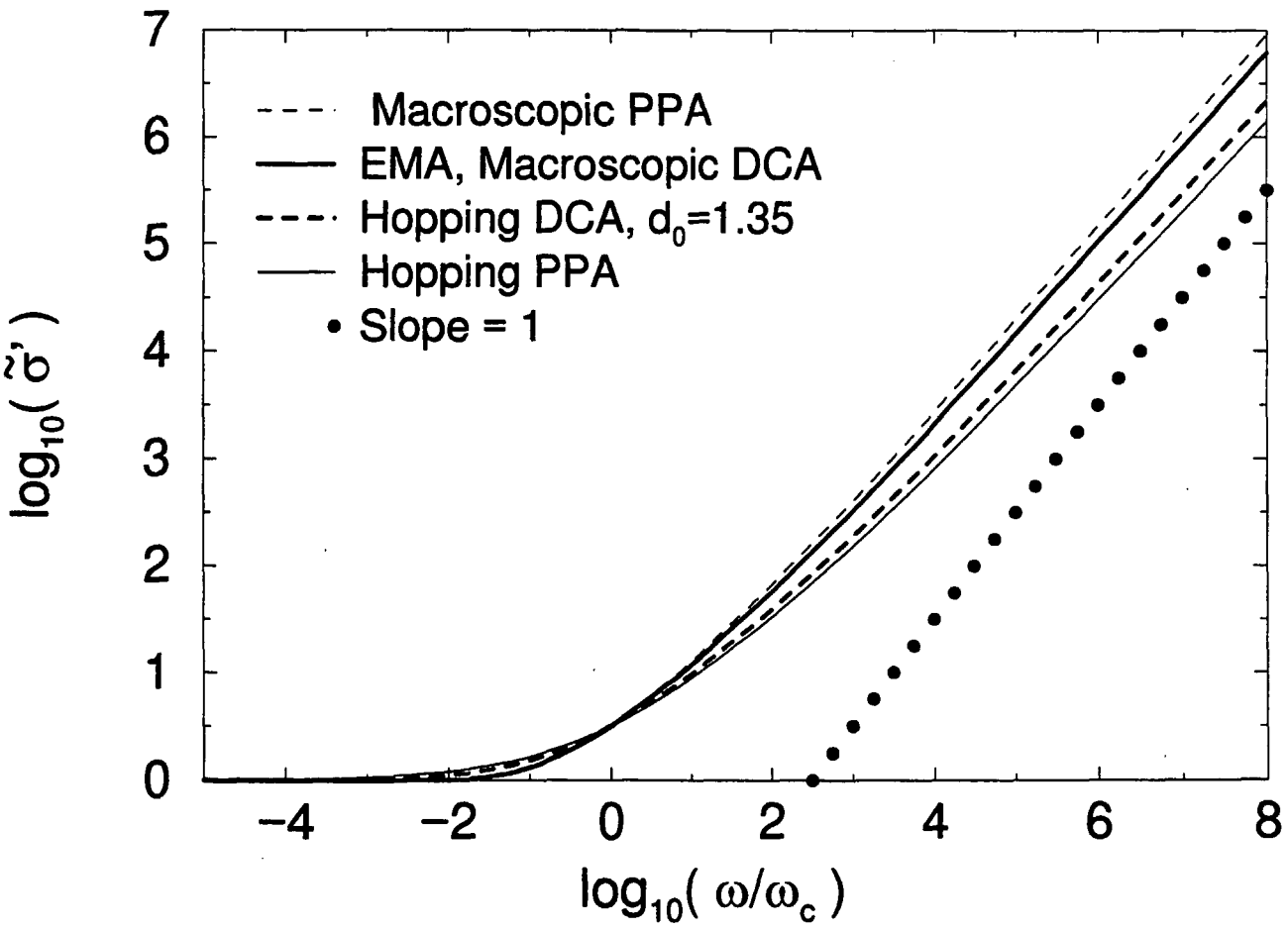
Macroscopic PPA
EMA, Macroscopic DCA
Hopping DCA, d_0=1.35
Hopping PPA
Slope = 1
$\log_{10}(\tilde{\sigma}')$
$\log_{10}(\omega/\omega_c)$
7
6
5
4
3
2
1
0
−4
−2
0
2
4
6
8

Fig. 11

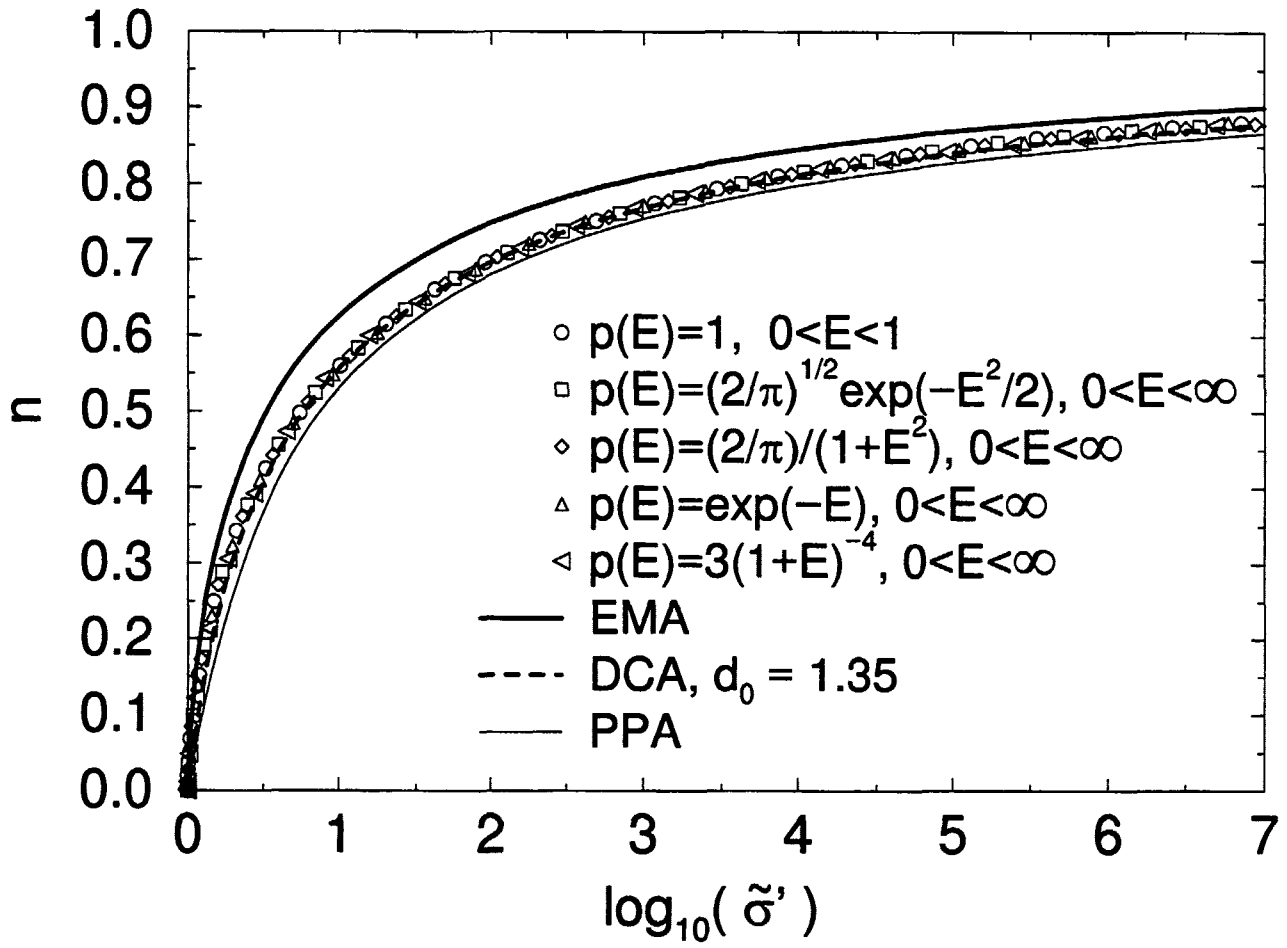
1.0
0.9
0.8
0.7
0.6
0.5
0.4
0.3
0.2
0.1
0.0
η
0
1
2
3
4
5
6
7
log10(σ̃')
p(E)=1, 0<E<1
p(E)=(2/π)^1/2 exp(−E^2/2), 0<E<∞
p(E)=(2/π)/(1+E^2), 0<E<∞
p(E)=exp(−E), 0<E<∞
p(E)=3(1+E)^−4, 0<E<∞
EMA
DCA, d0 = 1.35
PPA

Fig. 12(a)

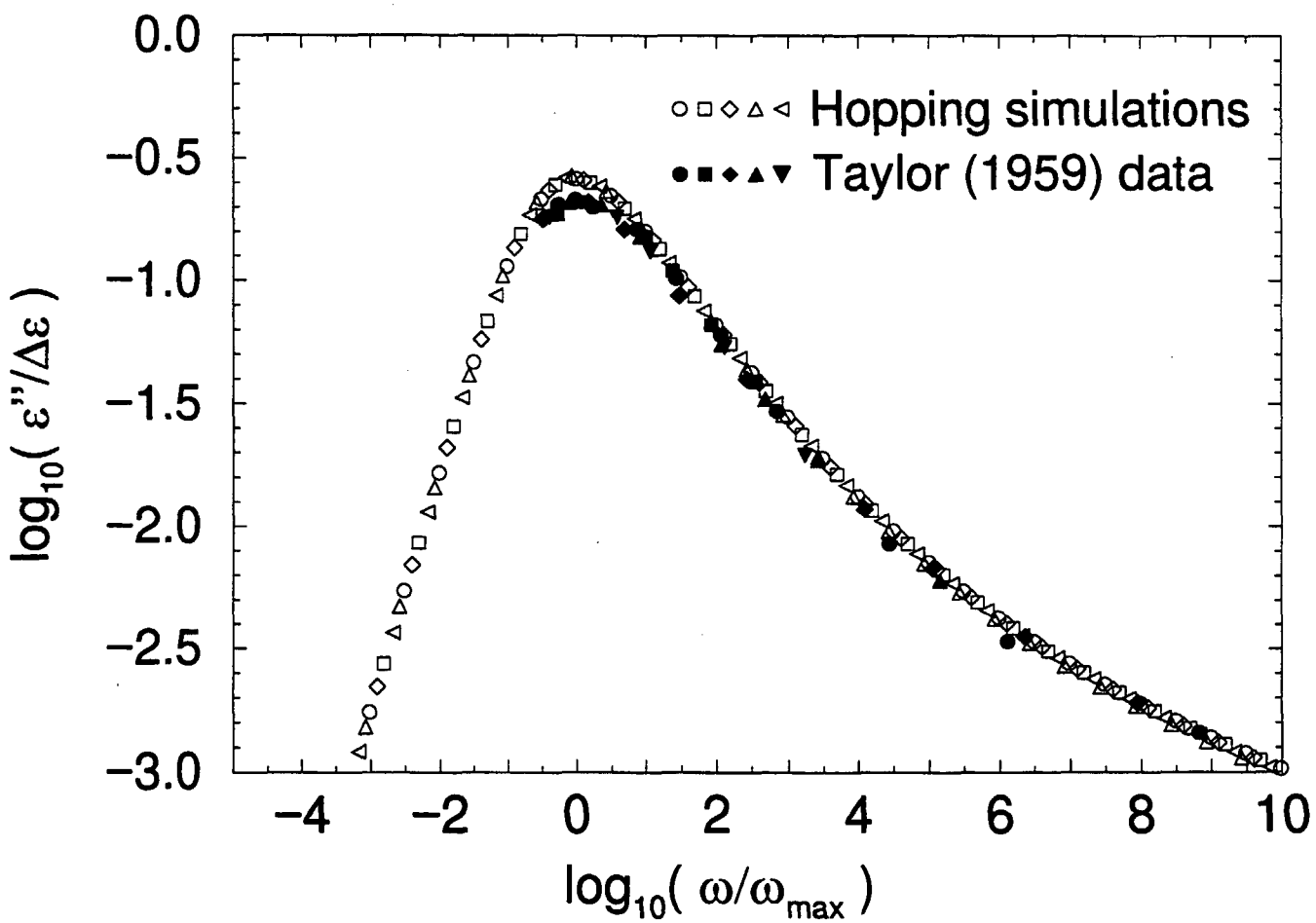
Hopping simulations
Taylor (1959) data
0.0
−0.5
−1.0
−1.5
−2.0
−2.5
−3.0
−4
−2
0
2
4
6
8
10
log10(ε''/Δε)
log10(ω/ωmax)

Fig. 12(b)

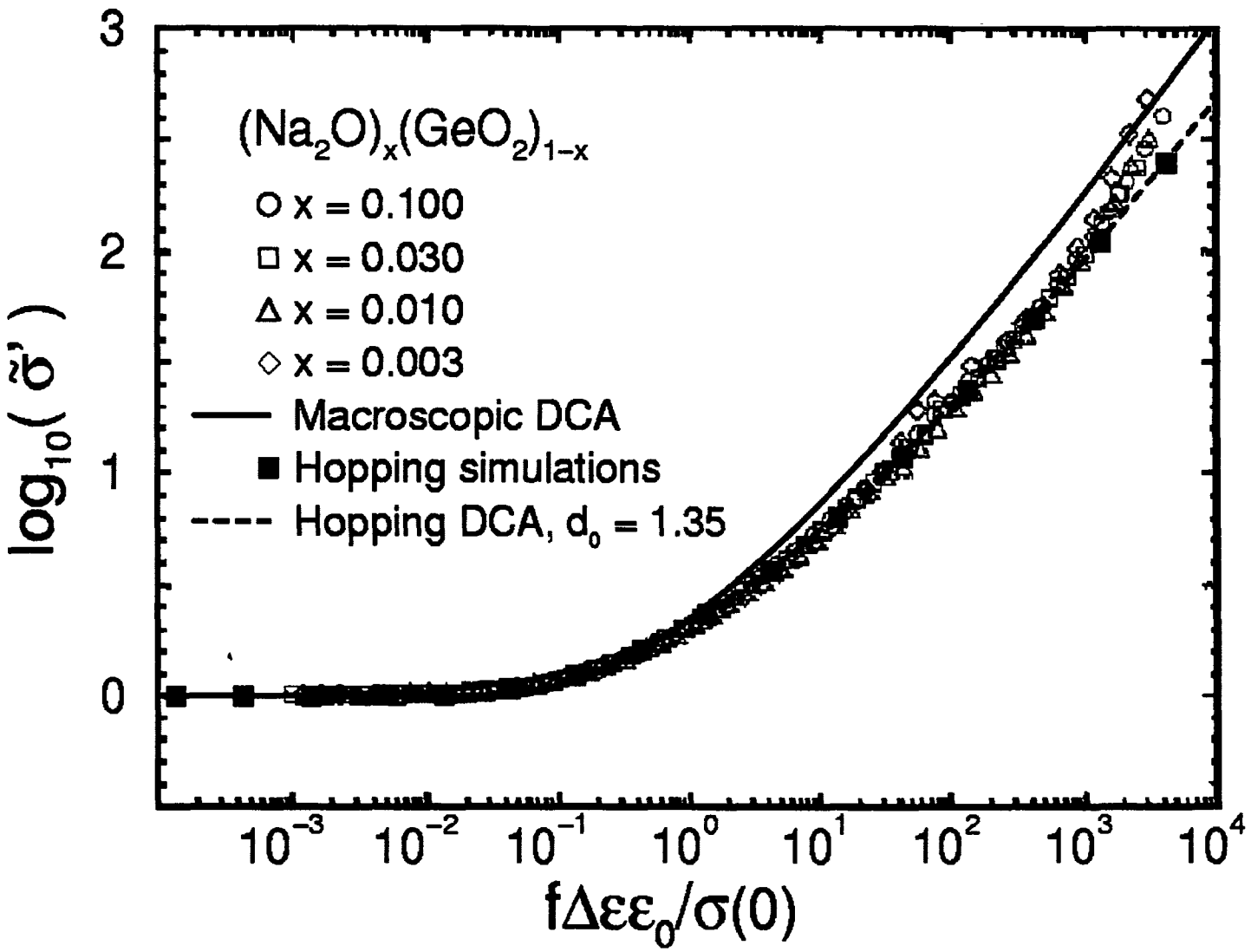
$(Na_2O)_x(GeO_2)_{1-x}$
x = 0.100
x = 0.030
x = 0.010
x = 0.003
Macroscopic DCA
Hopping simulations
Hopping DCA, $d_0 = 1.35$
$\log_{10}(\tilde{\sigma}')$
$f\Delta\varepsilon\varepsilon_0/\sigma(0)$
0
1
2
3
10^{-3}
10^{-2}
10^{-1}
10^{0}
10^{1}
10^{2}
10^{3}
10^{4}

Fig. 12(c)

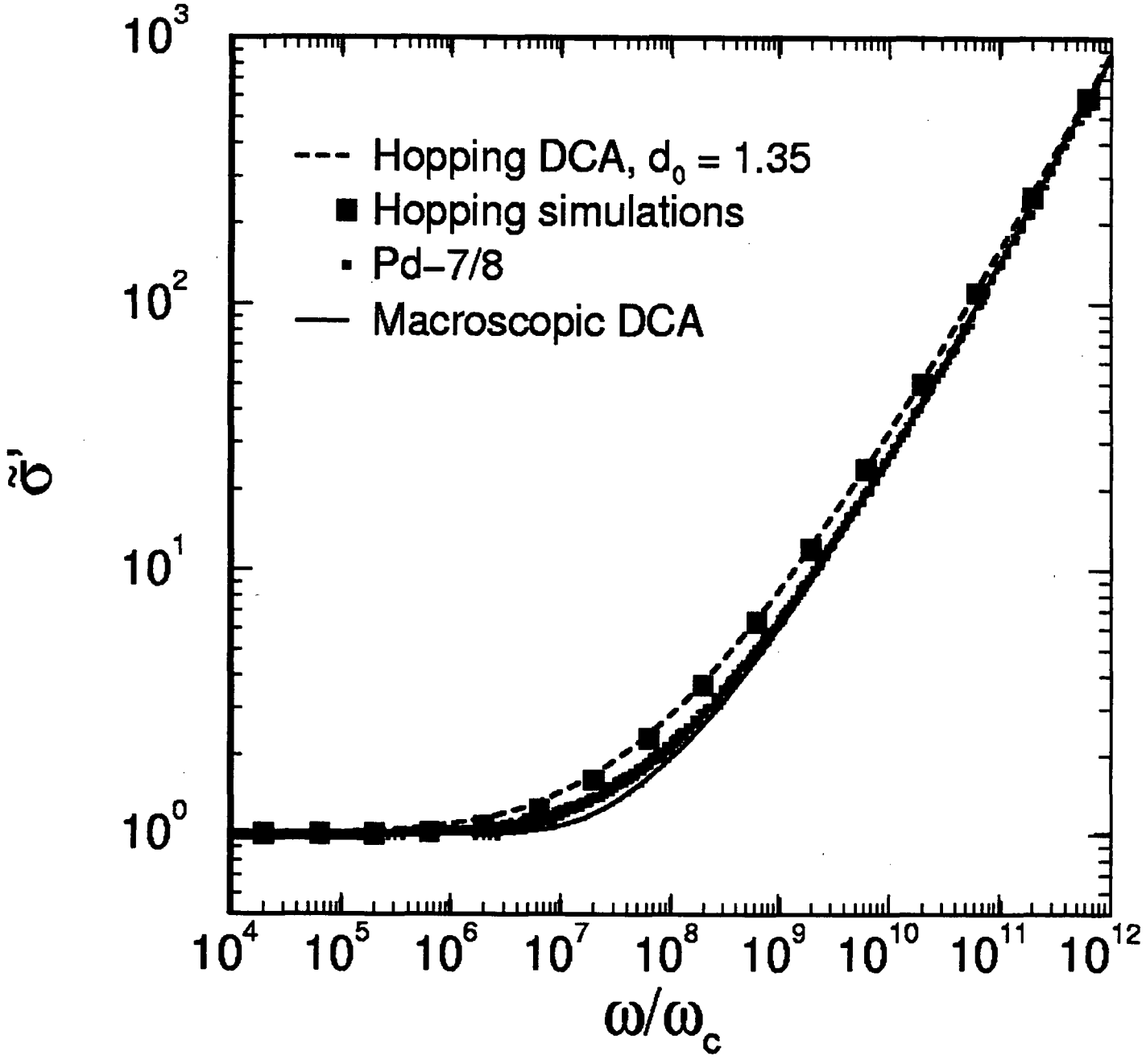
10^3
10^2
10^1
10^0
$\tilde{\sigma}$
--- Hopping DCA, $d_0 = 1.35$
■ Hopping simulations
▪ Pd–7/8
— Macroscopic DCA
10^4 10^5 10^6 10^7 10^8 10^9 10^{10} 10^{11} 10^{12}
ω/ω_c

Liste over tidligere udsendte tekster kan rekvireres på IMFUFA's sekretariat, tlf. 4674 2263 eller e-mail: bs@ruc.dk

332/97 ANOMAL SWELLING AF LIPIDE DOBBELTLAG
Specialerapport af:
Stine Sofia Korremann
Vejleder: Dorthe Posselt

333/97 Biodiversity Matters
an extension of methods found in the literature on monetisation of biodiversity
by: Bernd Kuemmel

334/97 LIFE-CYCLE ANALYSIS OF THE TOTAL DANISH ENERGY SYSTEM
by: Bernd Kuemmel and Bent Sørensen

335/97 Dynamics of Amorphous Solids and Viscous Liquids
by: Jeppe C. Dyre

336/97 PROBLEM-ORIENTATED GROUP PROJECT WORK AT ROSKILDE UNIVERSITY
by: Kathrine Legge

337/97 Verdensbankens globale befolkningsprognose
- et projekt om matematisk modellering
af: Jørn Chr. Bendtsen, Kurt Jensen, Per Pauli Petersen
Vejleder: Jørgen Larsen

338/97 Kvantisering af nanolederes elektriske ledningsevne
Første modul fysikprojekt
af: Søren Dam, Esben Danielsen, Martin Niss, Esben Friis Pedersen, Frederik Resen Steenstrup
Vejleder: Tage Christensen

339/97 Defining Discipline
by: Wolfgang Coy

340/97 Prime ends revisited - a geometric point of view -
by: Carsten Lunde Petersen

341/97 Two chapters on the teaching, learning and assessment of geometry
by Mogens Niss

342/97 LONG-TERM SCENARIOS FOR GLOBAL ENERGY DEMAND AND SUPPLY
A global clean fossil scenario discussion paper
prepared by Bernd Kuemmel
Project leader: Bent Sørensen

343/97 IMPORT/EKSPORT-POLITIK SOM REDSKAB TIL OPTIMERET UDNYTTELSE AF EL PRODUCERET PÅ VE-ANLÆG
af: Peter Meibom, Torben Svendsen, Bent Sørensen

344/97 Puzzles and Siegel disks
by Carsten Lunde Petersen

345/98 Modeling the Arterial System with Reference to an Anestesia Simulator
Ph.D. Thesis
by: Mette Sofie Olufsen

346/98 Klyngedannelse i en hulkatode-forstøvningsproces
af: Sebastian Horst
Vejledere: Jørn Borggren, NBI, Niels Boye Olsen

347/98 Verificering af Matematiske Modeller
- en analyse af Den Danske Eulerske Model
af: Jonas Blomqvist, Tom Pedersen, Karen Timmermann, Lisbet Øhlenschlæger
Vejleder: Bernhelm Booss-Bavnbek

348/98 Case study of the environmental permission procedure and the environmental impact assessment for power plants in Denmark
by: Stefan Krüger Nielsen
Project leader: Bent Sørensen

349/98 Tre rapporter fra FAGMAT - et projekt om tal og faglig matematik i arbejdsmarkedsuddannelserne
af: Lena Lindenskov og Tine Wedege

350/98 OPGAVESAMLING - Bredde-Kursus i Fysik 1976 - 1998
Erstatter teksterne 3/78, 261/93 og 322/96

351/98 Aspects of the Nature and State of Research in Mathematics Education
by: Mogens Niss

352/98 The Herman-Swiatec Theorem with applications

by: Carsten Lunde Petersen

353/98 Problemløsning og modellering i en almendannende matematikundervisning

Specialerapport af: Per Gregersen og Tomas Højgaard Jensen

Vejleder: Morten Blomhøj

354/98 A GLOBAL RENEWABLE ENERGY SCENARIO

by: Bent Sørensen and Peter Meibom

355/98 Convergence of rational rays in parameter spaces

by: Carsten Lunde Petersen and Gustav Ryd

356/98 Terrænmodellering
Analyse af en matematisk model til konstruktion af terrænmodeller
Modelprojekt af: Thomas Frommelt, Hans Ravnkjær Larsen og Arnold Skimminge
Vejleder: Johnny Ottesen

357/98 Cayleys Problem
En historisk analyse af arbejdet med Cayley problem fra 1870 til 1918
Et matematisk videnskabsfagsprojekt af:
Rikke Degn, Bo Jakobsen, Bjarke K.W. Hansen, Jesper S. Hansen, Jesper Udesen, Peter C. Wulff
Vejleder: Jesper Larsen

358/98 Modeling of Feedback Mechanisms which Control the Heart Function in a View to an Implementation in Cardiovascular Models
Ph.D. Thesis by: Michael Danielsen

359/99 Long-Term Scenarios for Global Energy Demand and Supply Four Global Greenhouse Mitigation Scenarios
by: Bent Sørensen

360/99 SYMMETRI I FYSIK
En Meta-projektrapport af: Martin Niss, Bo Jakobsen & Tune Bjarke Bonné
Vejleder: Peder Voetmann Christiansen

361/99 Symplectic Functional Analysis and Spectral Invariants
by: Bernhelm Booss-Bavnbek, Kenro Furutani

362/99 Er matematik en naturvidenskab? - en udspænding af diskussionen
En videnskabsfagsprojekt-rapport af Martin Niss
Vejleder: Mogens Nørgaard Olesen

363/99 EMERGENCE AND DOWNWARD CAUSATION
by: Donald T. Campbell, MArk H. Bickhard and Peder V. Christiansen

364/99 Illustrationens kraft
Visuel formidling af fysik
Integreret speciale i fysik og kommunikation
af: Sebastian Horst
Vejledere: Karin Beyer, Søren Kjørup

365/99 To know - or not to know - mathematics, that is a question of context
by: Tine Wedege

366/99 LATEX FOR FORFATTERE
En introduktion til LATEX og IMFUFA-LATEX
af: Jørgen Larsen

367/99 Boundary Reduction of Spectral invariants and Unique Continuation Property
by Bernhelm Booss-Bavnbek

368/99 Kvartalsrapport for projektet
SCENARIER FOR SAMLET UDNYTTELSE AF BRINT SOM ENERGIBÆRER I DANMARKS FREMTIDIGE ENERGISTYSTEM

Projektleder: Bent Sørensen

369/99 DYNAMICS OF Complex Quadratic Correspondences
by: Jacob Jalving

370/99 OPGAVESAMLING
Bredde-Kursus i Fysik 1976 - 1999
(erstatter tekst nr. 350/98

371/99 Bevisets stilling
- beviser og bevisførelse i en gymnasial matematikundervisning

Matematikspeciale af: Maria Hermannsson
Vejleder: Mogens Niss

372/99 En kontekstualiseret matematikhistorisk analyse af ikke-lineær programmering: udviklingshistorie og multipel opdagelse

Ph.d.-afhandling af Tinne Hoff Kjeldsen

373/99 Criss-Cross Reduction of the Maslov Index and a Proof of the Yoshida-Nicolaescu Theorem
by: Bernhelm Booss-Bavnbek, Kenro Furutani and Nobukazu Otsuki

374/99 Det hydrauliske spring
Et eksperimentelt studie af polygoner og hastighedsprofiler

Specialeafhandling af Anders Marcussen
Vejledere: Tomas Bohr, Clive Ellegaard, Bent C. Jørgensen